
JRC Scientific and Technical Reports



Calibration of PMP Condensation Particle Number Counters

Effect of material on linearity and counting efficiency

B. Giechaskiel, S. Alessandrini, F. Forni, M. Carriero, A. Krasenbrink
European Commission, Joint Research Centre, Transport and Air Quality Unit

J. Spielvogel, C. Gerhart
GRIMM AEROSOL Technik, GmbH & Co KG

X. Wang, H. Horn
TSI Incorporated

J. Southgate
AEA Energy & Environment

H. Jörgl
AVL List GmbH., Graz, Austria

G. Winkler
Technical University of Graz, Austria

L. Jing
Jing Ltd

M. Kasper
Matter Eng.

EUR 23495 EN - 2008

The mission of the Institute for Environment and Sustainability is to provide scientific-technical support to the European Union's Policies for the protection and sustainable development of the European and global environment.

European Commission
Joint Research Centre
Institute for Environment and Sustainability

Contact information

Alois Krasenbrink
Address: via Fermi 1
E-mail: alois.krasenbrink@jrc.it
Tel.: +39 0332 78 5474
Fax: +39 0332 78 9259

<http://ies.jrc.ec.europa.eu/>
<http://www.jrc.ec.europa.eu/>

Legal Notice

Neither the European Commission nor any person acting on behalf of the Commission is responsible for the use which might be made of this publication.

***Europe Direct is a service to help you find answers
to your questions about the European Union***

**Freephone number (*):
00 800 6 7 8 9 10 11**

(* Certain mobile telephone operators do not allow access to 00 800 numbers or these calls may be billed.

A great deal of additional information on the European Union is available on the Internet. It can be accessed through the Europa server <http://europa.eu/>

JRC 46963

EUR 23495 EN
ISBN 978-92-79-09766-9
ISSN 1018-5593
DOI 10.2788/95549

Luxembourg: Office for Official Publications of the European Communities

© European Communities, 2008

Reproduction is authorised provided the source is acknowledged

Printed in Italy

1. INTRODUCTION	3
2. EXPERIMENTAL	6
2.1 Instrumentation	6
Particle Generators	6
Electrometers	8
Particle Number Counters	8
Differential Mobility Sizers	8
Scanning Mobility Particle Sizers	9
Flowmeters	9
2.2 Set up	11
Measurement procedure	12
GRIMM – TSI comparison	13
2.3 Time schedule	14
2.4 Multiple charged particles effect	15
2.5 Safety precautions	17
3. GRIMM RESULTS	19
3.1 Size distributions of particles with different generators	19
3.2 Primary method	22
Linearity	22
Counting efficiency	24
3.3 Secondary method	26
Linearity	26
Counting Efficiency	27
Comparison of primary and secondary methods	29
4. TSI RESULTS	30
4.1 Size distributions of particles with different generators	30
Extra engine tests	32
4.2 Primary method	34
Linearity	34
Counting efficiency	37
4.2 Secondary method	41
Linearity	41
Counting Efficiency	41
5. DISCUSSION	43
5.1 Particle generators and material	43
5.2 Multiple charge effect	45
5.2.1 Size distributions and ε	45
5.2.2 Effect of ε on counting efficiencies	45
5.3 Electrometers	51
5.3.1 Electrometers stability	51

5.4 GRIMM-TSI comparability	52
5.4.1 Size distributions	52
5.5 Linearity and counting efficiency uncertainties	52
5.5.1 Repeatability	52
5.5.2 Reproducibility	54
5.6 Comparison with JRC's measurements	55
5.7 Comparison with other studies	56
6. SUMMARY & CONCLUSIONS	58
Primary method:	58
Linearity	58
Counting efficiency	58
Secondary method	59
Linearity	59
Counting efficiency	59
Uncertainties	59
Multiply charged particles effect	59
Key messages	60
Manufacturers (calibration)	60
Laboratories (validation)	60
7. REFERENCES	61
APPENDIX: SPECIFICATIONS OF EMERY OIL	62

1. INTRODUCTION

Recently the particle number method was proposed to the light duty regulation (Amendments Reg. 83). The particle number measurement system will consist of two main parts: the volatile particle remover (or sample preconditioning unit) and the particle number counter (PNC). The volatile particle remover is not examined in this report. The PNC shall:

- Operate under full flow operating conditions.
- Have a linear response to particle concentrations over the full measurement range in single particle count mode.
- Have a counting accuracy of ± 10 per cent across the range 1 cm^{-3} to the upper threshold of the single particle count mode of the PNC against a traceable standard. At concentrations below 100 cm^{-3} measurements averaged over extended sampling periods may be required to demonstrate the accuracy of the PNC with a high degree of statistical confidence.
- Have a readability of at least $0.1 \text{ particles cm}^{-3}$ at concentrations below 100 cm^{-3} .
- Have a data reporting frequency equal to or greater than 0.5 Hz .
- Have a T90 response time over the measured concentration range of less than 5 s .
- Incorporate a coincidence correction function up to a maximum 10% correction, and may make use of an internal calibration factor as determined in the calibration procedure, but shall not make use of any other algorithm to correct for or define the counting efficiency.
- Have counting efficiencies at particle sizes of $23 \pm 1 \text{ nm}$ and $41 \pm 1 \text{ nm}$ electrical mobility diameter of $50 \pm 12\%$ and $>90\%$ respectively. These counting efficiencies may be achieved by internal (for example; control of instrument design) or external (for example; size pre-classification) means.
- If the PNC makes use of a working liquid, it shall be replaced at the frequency specified by the instrument manufacturer.

The Technical Service shall ensure the existence of a calibration certificate for the PNC demonstrating compliance with a traceable standard within a 12 month period prior to the emissions test. The PNC shall also be recalibrated and a new calibration certificate issued following any major maintenance. Calibration shall be traceable to a standard calibration method:

- *Primary method:* By comparison of the response of the PNC under calibration with that of a calibrated aerosol electrometer when simultaneously sampling electrostatically classified calibration particles, or
- *Secondary method:* By comparison of the response of the PNC under calibration with that of a second PNC which has been directly calibrated by the above method.

In the electrometer case (primary method), calibration shall be undertaken using at least six standard concentrations spaced as uniformly as possible across the PNC's measurement range. These points will include a nominal zero concentration point produced by attaching HEPA filters of at least class H13 of EN 1822:1998 to the inlet of each instrument. With no calibration factor applied to the PNC under calibration, measured concentrations shall be within $\pm 10\%$ of the standard concentration for each concentration used, with the exception of the zero point, otherwise the PNC under calibration shall be rejected. The gradient from a linear regression of the two data sets shall be calculated and recorded. A calibration factor equal to the reciprocal of the gradient shall be applied to the PNC under calibration. Linearity of response is calculated as the square of the Pearson product moment correlation coefficient (R^2) of the two data sets and shall be equal to or greater than 0.97. In calculating both the gradient and R^2 the linear regression shall be forced through the origin (zero concentration on both instruments).

In the reference PNC case (secondary method), calibration shall be undertaken using at least six standard concentrations across the PNC's measurement range. At least 3 points shall be at concentrations below 1000 cm^{-3} , the remaining concentrations shall be linearly spaced between 1000 cm^{-3} and the maximum of the PNC's range in single particle count mode. These points will include a nominal zero concentration point produced by attaching HEPA filters of at least class H13 of EN 1822:1998 to the inlet of each instrument. With no calibration factor applied to the PNC under calibration, measured concentrations shall be within $\pm 10\%$ of the standard concentration for each concentration, with the exception of the zero point, otherwise the PNC under calibration shall be rejected. The gradient from a linear regression of the two data sets shall be calculated and recorded. A calibration factor equal to the reciprocal of the gradient shall be applied to the PNC under calibration. Linearity of response is calculated as the square of the Pearson product moment correlation coefficient (R^2) of the two data sets and shall be equal to or greater than 0.97. In calculating both the gradient and R^2 the linear regression shall be forced through the origin (zero concentration on both instruments).

Calibration shall also include a check on the PNC's detection efficiency with particles of 23 nm electrical mobility diameter. A check of the counting efficiency with 41 nm particles is not required.

There is one open issue on the calibration procedures of the PNCs and this is the selection of the material. Proper selection of the test aerosol is essential to instrument calibration. The PNCs counting efficiency strongly depends on the properties of the aerosol particles, thus the calibration curve is strictly valid for the test aerosol (Kulmala et al. 2007). It has been also shown that the material dependence is greater for PNCs with lower temperature differences between the saturator and the condenser (Wang et al. 2007). Another issue is whether PNCs from different manufacturers are comparable, since different aerosol materials are used for calibration (e.g. emery oil from TSI and NaCl from GRIMM). Thus it would be desirable to use a generally accepted calibration material. However, as the PNCs are used to measure diesel aerosol, a material with similar behaviour with diesel soot should be used also for the calibration. As the diesel aerosol depends on many parameters (e.g. engine, engine load, fuel etc) and can contain a wide range of materials (e.g. soot, sulphuric acid, hydrocarbons etc) the main target of this study was not to identify the material with exactly the same behaviour as diesel aerosol, but similar. In addition, another target was to comment on the proposed PNC calibration procedures concerning correctness, completeness and applicability. Finally it was desired to qualify uncertainties of the calibration factors between different companies. During 3rd-7th December 2007 a workshop was organised by Joint Research Centre (JRC, Ispra, Italy) of the European Commission to address these issues.

GRIMM and TSI provided PNCs and AEA, MATTER, GRIMM, TSI provided five particle generators (evaporation-condensation, electrospray, CAST). The experiments were conducted in the European's Commissions laboratories (JRC). Heavy duty diesel engine (w/o aftertreatment) particles were also produced (measurements downstream a thermodenuder) at idle and a medium load mode. The measured data were evaluated by JRC.

2. EXPERIMENTAL

2.1 Instrumentation

Particle Generators

The characteristics of an ideal generator are a constant and reproducible output of stable aerosol particles whose size and concentration can be easily controlled. The generators used in this workshop were:

Evaporation-condensation technique: In this method the heated vapour substance is mixed with nuclei on which it subsequently condenses when it passes in laminar flow through a cooling zone (Figure 1). AEA used this method to generate NaCl and C40 (tetracontane) particles. The aerosol generator consisted of a ceramic crucible heated via an electric Bunsen. The bulk material (NaCl or C40) was placed in the ceramic crucible and heated to near its boiling point. A small flow was introduced into the crucible to displace vapour from the surface of the bulk material to a cooler region of the generator where condensation occurred. Particle diameters could be varied by controlling the rate of vapour transport from the crucible (via the crucible air flow) and/or the subsequent cooling rate of the vapour (via the carrier air flow).

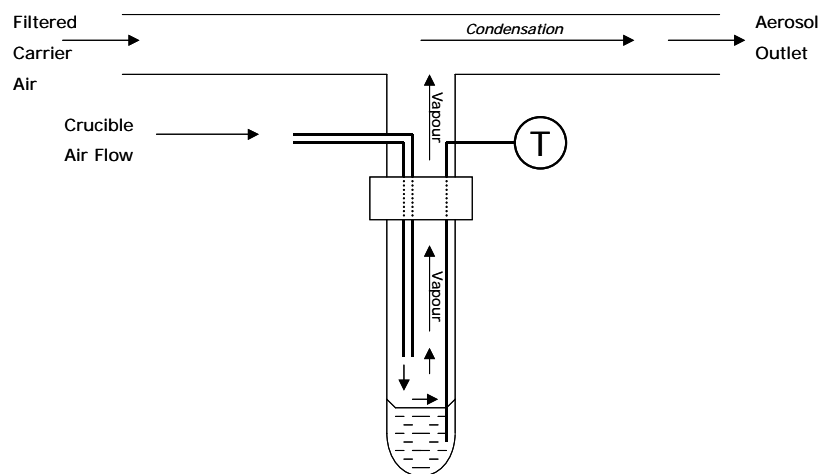


Figure 1: Evaporation – condensation technique.

Electrospray technique: This method refers to the generation of liquid droplets by feeding a liquid solution or suspension through a capillary tube and applying an electrical field to liquid at the capillary tip (Figure 2). The electrical field draws the liquid from the tip into a conical jet from which ultrafine charged droplets are emitted. Air and CO₂ are merged with the droplets, and the liquid evaporates while the charge is neutralized by an ionizer. The result is a neutralized, monodisperse aerosol that is practically free of solvent residue. TSI uses this method to electro spray emery oil (Emery 3004 or PAO 4 cSt), a highly branched isoparaffinic polyalphaolefin (1-decene (tetramer) mixed with 1-decene (trimer), hydrogenated, see Annex) for PNC calibration. It is supposed to provide spherical particles of chemical composition representative of synthetic lube oil particles.

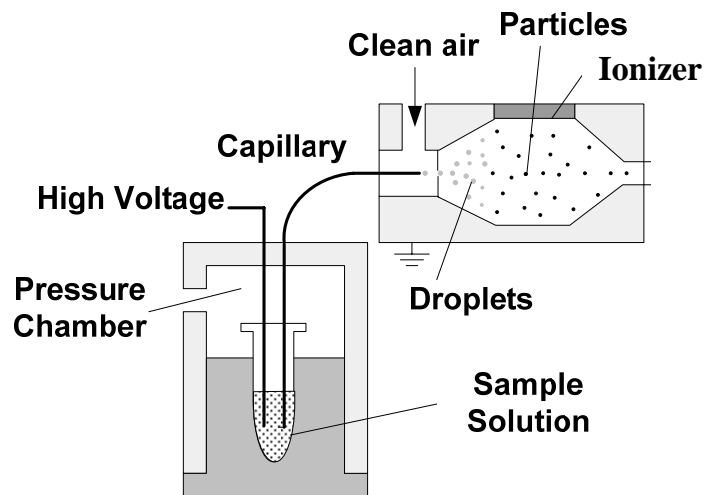


Figure 2: Electro-spray technique.

CAST (Combustion Aerosol Standard): The soot generators use a diffusion flame to form soot particles during pyrolyse (Figure 3). Within the soot generating burner the flame is mixed with quenching gas at a definite flame height. As a consequence the combustion processes are quenched and a particle flow arises out of the flame and leaves the combustion chamber. Sufficient quenching stabilizes soot particles and inhibits condensation in the particle stream when it escapes from the flame unit into the ambient air condition. Subsequently air is supplied to dilute the particle stream. For operation the gas inlets are connected through flow restrictors or flow controllers respectively, to the corresponding gas sources. The state of the flame and the features of generated soot particles respectively are primarily given as a result of the flow settings. By means of varying the flow settings the particle size can be adjusted in a predefined range of particle size, e.g. 10 to 50 nm. The flame supplies soot particles within a range of $10^6 - 10^7$ particle/cm³. These are diluted by quench gas and as an option, subsequently by adding dilution air. The mini-CAST generator from GRIMM and the CAST generator from Matter Eng. were used. The flowrates used are: C₃H₈ 10 mlpm, Air 220 mlpm, N₂ 1 lpm, air 1 lpm.

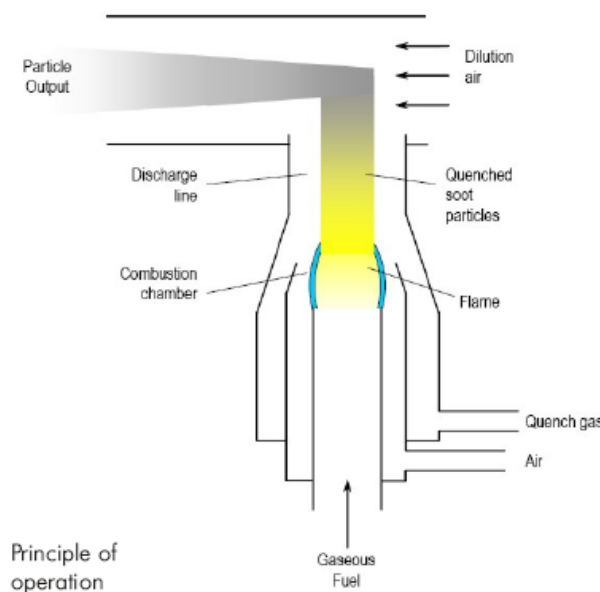


Figure 3: CAST generator principle of operation.

Diesel soot: An INEVCO Cursor 8 heavy duty engine without any after-treatment was used as diesel soot source. For the tests on the 05/12/2007 instruments were sampling downstream an ejector dilutor (Dekati Ltd) and a thermodenuder at 250°C (Dekati Ltd) connected at CVS. The CVS flowrates at idle and 2000rpm/600Nm were 60 and 100 m³/min. For the measurements of 6/12/2007 (only idle) the instruments were sampling through the HC line (without any filter) and a thermodenuder. The residence time in this line was estimated 2.5 s (plus 3 s in the thermodenuder). On the 07/12/2007 (engine at 2000rpm/600Nm) the instruments were sampling from the HC line without the thermodenuder, but downstream an ejector dilutor to reduce the pressure pulsations.

Electrometers

The GRIMM model 5.705 electrometer is a primary standard that measures the charge on aerosol particles of the size 0.8 to 700 nm. The charge is measured in a Faraday Cup where the charge initiates a small current that is converted to a voltage using a 1 TΩ resistor. This is an absolute method that requires no calibration, still spot checking is performed with our in-house primary standard. It is important to know the exact value of the resistor that is supplied by the manufacturer and the flow that is calibrated with a NIST traceable flow meter. The noise of the GRIMM electrometer is 0.25 fA (19 elementary charges/cm³) at 5 l/min sample flow.

The TSI 3068B electrometer measures total net charge on aerosol particles from 0.002 to 5 μm. It has a sensitivity of ±1 fA, with a dynamic range of ±12500 fA. It has been compared against the Japanese AIST aerosol electrometer standard and shown equivalent efficiency. However, during the measurement, it was found that 3068B aerosol electrometer consistently read ~7.3% higher than the 3776 Condensation Particle Counter for emery oil particles. Due to a tight experiment schedule, no effort was spent to debug which one is more accurate. Since the electrometer was more susceptible to uncertainties due to shipping and handling, the 3776 UCPC concentration was considered more reliable, and thus the AE concentration was reduced by 7.3% for all data reported in this document.

Particle Number Counters

GRIMM used one PNC (model 5.403 S/N: 003) with cut-point 4.5 nm (as a reference PNC for the secondary calibration method) (owned by JRC) and two PNCs (model 5.404 S/N: 412, 608) with cut-points at 23 nm. All PNCs were run at 1.5 lpm. All PNCs were calibrated using NaCl particles nebulised. Note that the specifically developed GRIMM PMP-CPC 5.430 is calibrated with soot particles from the mini-CAST.

TSI's PNCs with d₅₀ at 23 nm (calibrated using emery oil particles) included the old golden CPC 3010D, the new CPC 3790 (JRC) and another 3790 (TSI). A 3776 and a 3025A (owned by JRC) were also used as reference instruments for the secondary method (d₅₀ at 3 nm, calibrated with sodium chloride particles as they are less evaporative).

Before the any measurement new butanol was added to all PNCs.

Differential Mobility Sizers

GRIMM used a Vienna-Type M-DMA (5 to 350 nm) that has been shown (Reischl et al. 1997) to feature excellent resolution and very small losses for smallest particles. It was controlled and set to the specified sizes with a DMA-Controller. TSI used a 3081 electrostatic classifier (owned by JRC) with a nano-column (owned by TSI) (called nano-DMA).

Scanning Mobility Particle Sizers

At the beginning of the tests for each material GRIMM and TSI measured the size distributions to check their suitability (mean and concentration of the peak) for the linearity and counting efficiency tests with scanning mobility particle sizers (SMPS). Sometimes the size distributions were also measured at the end of the tests to check the stability of the generators. GRIMM used a SMPS+E (a second M-DMA with a FCE). TSI used the nano-DMA 3085N with the 3776 PNC (called nSMPS).

Flowmeters

For the measurement of the PNCs' flowrates a soap bubble meter (mini-BUCK Calibrator M-5) was used (1-6000 cc/min) with a $\pm 0.5\%$ accuracy of the display reading. The last certified calibration was in Apr 04, however regular checks in-house were performed with Sierra Instruments 820 Mass Flow Meter Model 821-1-PE, S/N: 3259 (last calibrated Nov 07). For the ambient temperature and pressure measurement a TSI 4040 flow meter was used. The uncertainty is ± 1 kPa and $\pm 1^\circ\text{C}$.

Table 1 summarises the equipment used.

Table 1: Summary of equipment used during the calibration workshop. Date in parenthesis shows the last calibration of the specific equipment.

<i>Instrument</i>	<i>Comp.</i>	<i>Model</i>	<i>S/N</i>	<i>Comments</i>
<i>Flowmeters</i>				
Flowmeter	BUCK	M-5	052795 (*)	Volumetric flow meter
Flowmeter	TSI	4040E	4040 0729 025 (23 Jul 07)	For ambient temperature and pressure. Owned by JRC.
<i>Particle Generators</i>				
Engine diesel soot generator	IVECO	Cursor 8	-	PMP HD "golden engine" w/o any aftertreatment.
NaCl generator	AEA		-	Prototype evaporation-condensation generator
C40 generator	AEA		-	Prototype evaporation-condensation generator
Electrospray	TSI	3480	70515032	Commercially available
CAST	JING	CAST 2	100 907	Owned by MATTER
Mini-CAST	JING	Mini-CAST	001	Prototype soot generator owned by GRIMM

<i>GRIMM instrumentation</i>				
FCE Electrometer	GRIMM	FCE 5.705	57050503 (Jul 2007)	Reference for primary calibration method
M-DMA Electrostatic classifier	GRIMM	M-DMA	5UP60501 (Apr 2007)	Size range 5-350 nm with DMA controller (57060503)
Neutraliser	GRIMM	Am 241		Owned by JRC
SMPS-E Scanning Mobility Sizer	GRIMM	M-DMA DMA contr. FCE 5.705	5UP60710 (May 2008) 57060702 (May 2008) 57050704 (Oct 2007)	For size distributions in the range 5-350 nm. The neutraliser was supplied from JRC (Am 241)
PNC 003	GRIMM	5.403	54011003 (Oct 2004)	Reference for secondary calibration method. Owned by JRC.
PNC 412	GRIMM	5.404	54300412 (Jul 2007)	PMP settings.
PNC 608	GRIMM	5.404	54300608 (Jun 2007)	PMP settings. With environmental sensor (3KE20705)
<i>TSI instrumentation</i>				
Nano-DMA Electrostatic classifier	TSI	El. classif. 3085N	8029 (19 Jun 07) 70424125	Size range 3-165 nm. El. Class. supplied by JRC, nano column by TSI.
AE Electrometer	TSI	3068B AE	70601289 (8 Nov 07)	Reference for primary calibration method
nSMPS Scanning Mobility Sizer	TSI	El. classif. 3085N 3776	8029 70424125 70530186	For size distributions in the range 3-165 nm.
PNC 3010D	TSI	3010D	70515208 (14 Oct 05)	PMP settings. Provided by JRC. Old Golden PNC
PNC TSI 3790	TSI	3790	70644199 (13 Jan 06)	PMP settings.
PNC JRC 3790	TSI	3790	70721012 (20 Jun 07)	PMP settings. Provided by JRC.
PNC 3776	TSI	3776	70530186 (22 Mar 07)	Reference for secondary calibration method.
PNC 3025A	TSI	3025A	1400 (13 Jun 07)	Provided by JRC. Recently calibrated

2.2 Set up

The schematic of the GRIMM and TSI set up can be seen in Figure 4 and Figure 5 respectively.

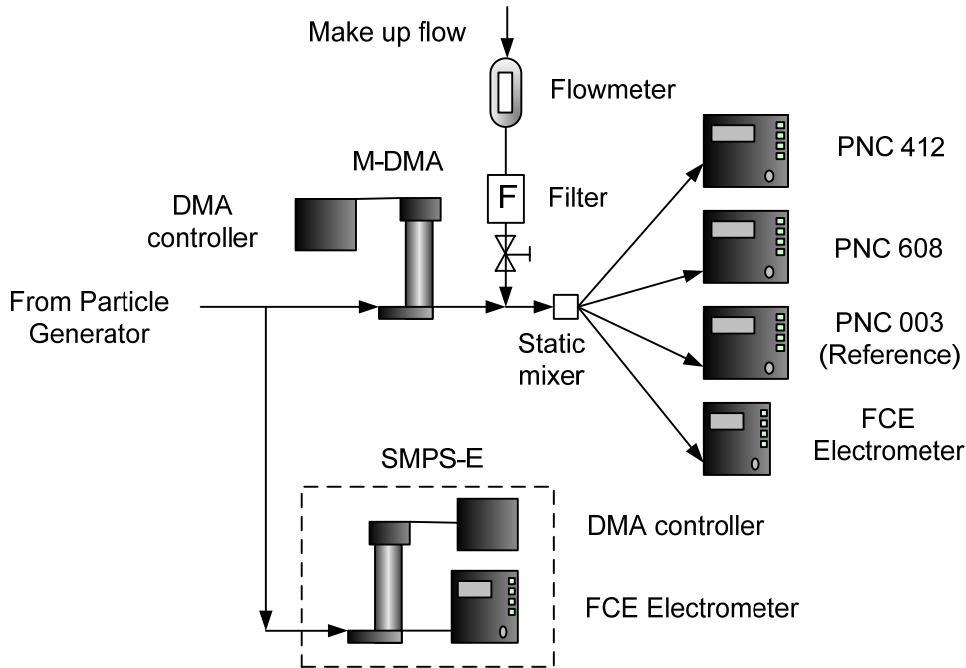


Figure 4: GRIMM set up.

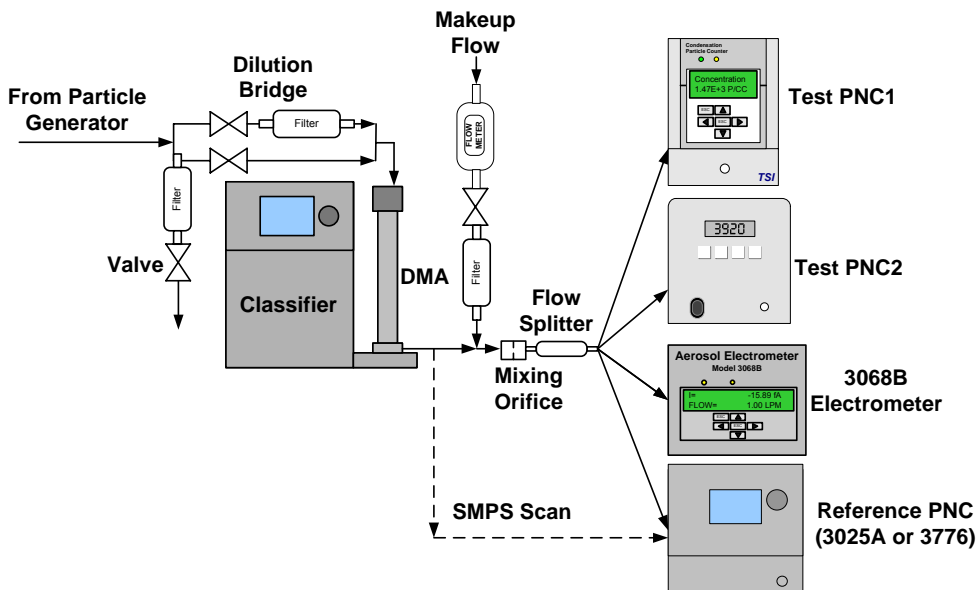


Figure 5: TSI set up.

Test aerosols were generated using the particle generation systems described previously. The polydisperse aerosol from the generator first passed through a dilution bridge (only for the TSI set up), which controlled the aerosol concentration. Next, the differential mobility analyzer (DMA) and the classifier selected particles of a given mobility diameter. The sheath to aerosol flow ratio of the DMA was typically set at 10:1 to ensure a narrow “monodisperse” size distribution. Filtered makeup flow was added downstream of the DMA to maintain a flow balance. A mixing orifice was used to enhance the turbulent mixing and ensure uniform aerosol concentration. The aerosol flow then split to the test PNCs and the

Aerosol Electrometer. In order to keep the particle diffusional losses the same, the residence time in the tubes from the splitter to the PNC/Electrometer inlet were the same. The tubes used had also the same inner diameter, as the diffusion losses do not depend on the tube diameter for a given volumetric flow (Hinds 1999).

Before the beginning and after the end of the measurements the DMA combined with a PNC was measuring the size distribution (in the case of GRIMM, the SMPS-E was measuring in parallel).

The flowrates of the PNCs (of both GRIMM and TSI) were measured with a soap bubble meter M-5 only once at the beginning of the workshop. It was also ensured that the test aerosol pathways to each instrument were equivalent (similar residence times). The ambient temperature and pressure, which were measured with a 4040 TSI flowmeter, remained constant during the measurements ($21.5 \pm 1^\circ\text{C}$ and $98.5 \pm 1.5 \text{ kPa}$ respectively). The flow rates were not taken into account in the PNC results because it was desired to include in the slope the flow rate effect. Thus the user will have to correct with one number and not with two his number results.

Table 2: Instruments' flowrates (measured with the same flowmeter M-5 Buck).

<i>FCE</i>	<i>003</i>	<i>412</i>	<i>608</i>	<i>AE</i>	<i>3010D</i>	<i>JRC 3790</i>	<i>TSI 3790</i>	<i>3776</i>	<i>3025A</i>
1.501	1.489	1.494	1.502	0.999	1.003	0.988	1.012	1.000	-



Figure 6: An overview of the setup.

Measurement procedure

The following calibration procedure was followed in most measurements (for both companies):

- A filter was connected at the test instrument inlets to ensure PNC zero counting and AE (FCE) zero current offset.

- The DMA controller / classifier was set in the SMPS scan mode to measure particle size distributions from the aerosol generator. The measurements did not initiate until the distribution was more or less stable (three consecutive scans were similar by the eye). The generator was adjusted to create a new size distribution if necessary.
- Doubly charge fraction was measured with the DMA controller / classifier when set at a defined voltage. In sequence, the classifier was set to measure 23 nm, 41 nm, and a larger size for linearity measurement. The reference PNC (TSI 3776) concentrations were recorded. Then the voltages of the corresponding sizes were doubled and again the reference PNC concentrations were recorded. The generator was adjusted to create a new size distribution if necessary.
- The classified aerosol was connected to the test instruments, the make up flow and the dilution bridge were adjusted to achieve the desired concentrations. It was ensured that the DMA aerosol to sheath ratio was not greater than 1:5. The maximum mobility range of particles exiting the DMA is $Z^* \pm 0.2Z^*$, where Z^* is the DMA centroid mobility. This corresponds to a size range of 21.0-25.7 nm for 23 nm, 37.4-45.9 nm for 41 nm, 54.7-67.2 nm for 60 nm.
- No leakages were ensured when all instruments were connected and the voltage at the DMA controller / classifier was 0V.
- The counting efficiencies of 23 nm and 41 nm were measure at concentrations of $\sim 4000 \text{ cm}^{-3}$.
- The linearity was measured at a larger size at concentrations of 10000, 8000, 6000, 4000, 2000, and 0 cm^{-3} . Each data point was recorded for 2 minutes at 1 Hz data acquisition rate.
- For the linearity check with the secondary method one particle diameter (50-120 nm) was chosen and the concentration was changed with a diluter upstream or downstream the classifier. This method was preferred as the results would be comparable with the primary method.

This method takes the PNC and electrometer readings once per second for about 120 seconds, and uses the averaged concentrations to calculation the PNC counting efficiency. The Japanese AIST method alternatively turns the DMA voltage on/off for one minute, and repeats each measurement for 3 times. The electrometer zero offset measured when the DMA voltage is off is subtracted from each measurement to reduce the uncertainties due to electrometer drift. The AIST method is more accurate. It however, takes longer time (6 minutes for each measurement). The method used in this workshop is faster (2 minute for each measurement), but is less accurate if the electrometer drifts. The faster method was used in the workshop except the runs named EO-AIST.

GRIMM – TSI comparison

For a direct comparison between the two companies, TSI supplied the Electro spray to produce Emery Oil particles. GRIMM provided the M-DMA for the classification of particles. The FCE and the PNC model 5.404 S/N: 608 from GRIMM and the AE and the JRC 3790 from TSI were sampling in parallel. Only counting efficiency at 23nm and at 41nm was measured. The setup can be seen in Figure 7.

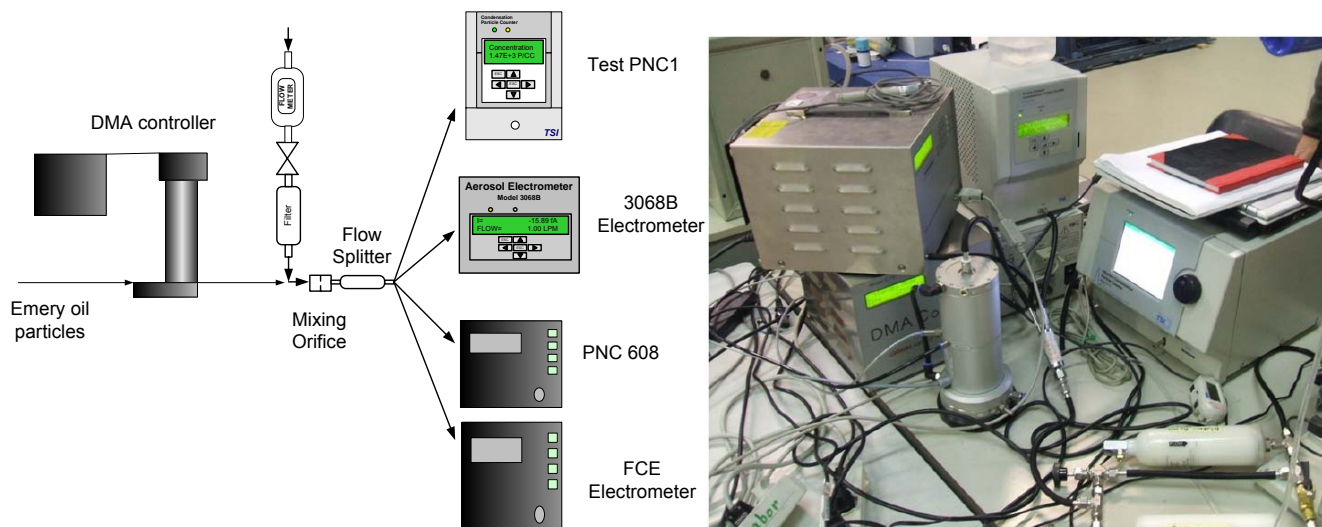


Figure 7: Setup of TSI and GRIMM comparison and overview.

2.3 Time schedule

The time schedule of the measurements can be seen in Table 3. The first day the companies setup their instrumentation (03/12/2007). Second and third days were mainly used for the calibration of the PNCs (04 and 05/12/2007). The last two days TSI made some extra tests and repetitions.

Table 3: Time schedule of PNC calibration workshop in JRC VELA-5.

Day	Material	Companies
03/12/2007	Set up	TSI, GRIMM
	Set up	TSI, GRIMM, AEA, JING
04/12/2007	NaCl	TSI, GRIMM, AEA, JING
	mini-CAST, C40	TSI, GRIMM, AEA, JING
05/12/2007	Diesel soot, emery oil, CAST	TSI, GRIMM, AEA, JING, MATTER
	Volatile Removal Efficiency (C40)*	TSI, GRIMM, AEA, JING, MATTER
06/12/2007	Particle Reduction Factor (NaCl)*	TSI, AEA
	Diesel soot	TSI
07/12/2007	Emery oil	TSI
	Diesel soot	TSI

* The results from the volatile removal efficiency and particle reduction factor will be presented elsewhere.

2.4 Multiple charged particles effect

An aerosol with a narrow range can be produced by passing a polydisperse aerosol through a size classifier. Commonly a differential electrical mobility analyser is used to classify particles of the same mobility. Because most of the classified particles are singly charged, most of the aerosol produced is monodisperse, but there is a smaller amount of doubly charged particles with the same electrical mobility but different particle size (bigger).

The multiply charged particle fraction can vary significantly among the different aerosol generation techniques. The multiply charged particles have a two fold effects:

- The electrometer overestimates particle concentration due to more current generated by multiply charged particles. This can lead to low test PNC linearity slopes and lower test PNC counting efficiency.
- The test PNCs seem to have higher counting efficiency because the multiply charged particles are physically larger than the singly charged particles with the same mobility diameter (and PNCs have better efficiency for bigger particles).

The contribution of these effects is difficult to precisely calculate, so the multiply charged fractions should be minimised. One rigorous way to correct the experimental error due to multiple charging is to carry out a Tandem Differential Mobility Analysis (TDMA) experiment to determine the fraction of multiply charged particles and correct the efficiency data. One simpler way to minimize the multiple charging effects is to sample the test “monodisperse” aerosol from the right-hand side of the mode of the polydisperse aerosol from the generator. In that case, the polydisperse particle size distribution is first scanned with the DMA connected to a reference PNC (i.e., a SMPS system). And then the DMA voltage is set to select the test aerosol from the right-hand side of the size distribution. This procedure was followed for the measurements described in this report.

In addition, TSI used the following steps to estimate multiple charge fractions:

- A PNC_A with low cut size (e.g. 3776) was used to measure the particle concentration (n_1') of single charged size (d_1) at DMA voltage at V.
- Then the doubly charged size (d_2) concentration (n_2') was measured at double voltage (2V).
- Assuming no multiply charged particle contamination at d_2 , the concentration of doubly charged particle at DMA voltage of V will be $n_2 = n_2' f_2 / f_1$, where f_2 and f_1 are the doubly and singly charge probabilities of size d_2 (see e.g. Table 5).
- The singly charge particle concentration is $n_1 = n_1' - n_2$, assuming no particles are more than doubly charged.
- The ratio of doubly and singly charged fraction is then:

$$\varepsilon = n_2 / n_1 \quad (\text{Eq. 1})$$

To correct the doubly charged effect for the PNC counting efficiency the following steps were followed:

- PNC_B under calibration (with cut size c_1 at d_1 and c_2 at d_2) and AE measured the concentrations at DMA voltage V.

- The concentration that the PNC_B measures is:

$$N_{CPC} = n_1 c_1 + c_2 n_2 \quad (\text{Eq. 2})$$

- The current that the AE measures is:

$$I_{AE} = eQ(n_1 + 2n_2) \quad (\text{Eq. 3})$$

- Combining Eq. 1-3 the corrected counting efficiency of the PNC_B at d_1 is:

$$c_1 = \frac{N_{CPC} - c_2 \frac{I_{AE}}{eQ} \frac{\varepsilon}{1+2\varepsilon}}{\frac{I_{AE}}{eQ} \frac{1}{1+2\varepsilon}} \quad (\text{Eq. 4})$$

In deriving Eq. 4, it was assumed that:

- Only singly and doubly charged particles are present at V. For diameters <100 nm this assumptions is almost always valid.
- At 2V, all particles are singly charged. For diameters <100 nm this assumptions is almost always valid.
- The counting efficiency of d_2 is c_2 , which was usually set as 1 (Eq. 2).

It can be observed from Eq. 2 and 3 that the multiple charge effect increases the concentration that the PNC and the electrometer measure:

$$\text{PNC overestimation: } \frac{c_2}{c_1} \varepsilon \quad (\text{Eq. 5})$$

$$\text{AE overestimation: } 2\varepsilon \quad (\text{Eq. 6})$$

In case that $\varepsilon=0$, Eq. 4 becomes:

$$c_1 = \frac{N_{CPC}}{\frac{I_{AE}}{eQ}} \quad (\text{Eq. 7})$$

In case that $\varepsilon \neq 0$, then without any correction the measured counting efficiency would be:

$$c_{1,m} = \frac{N_{CPC}}{\frac{I_{AE}}{eQ}} \quad (\text{Eq. 8})$$

Similarly, to estimate the effect for the secondary method the number concentration that the reference CPC measures (as in Eq.5) is:

$$N_{CPC,ref} = n_1 + n_2 \quad (\text{Eq. 9})$$

Then the counting efficiency of the test CPC, combining Eq. 1, 2 and 9 is:

$$c_1 = (1 + \varepsilon) \frac{N_{CPC}}{N_{CPC,ref}} - \varepsilon \quad (\text{Eq. 10})$$

Reference CPC overestimation: ε (Eq. 11)

In case that $\varepsilon \neq 0$ and no corrections are conducted, the measured counting efficiency will be:

$$c_{1,m} = \frac{N_{CPC}}{N_{CPC,ref}} \quad (\text{Eq. 12})$$

An estimation of the multiply charged particles is given in the “Discussion” section, based on the above equations.

In the following results, the AE reading was corrected for the zero (background) levels and its flow rate (although negligible correction). TSI AE was also corrected -7.3% (see section 2.1) The PNC 3010D was corrected for coincidence. The PNCs were not corrected for their flow rate. The results presented are not corrected for multiple charged particles. Their effect will be discussed in section 5.

The values used to calculate f_i are shown in Table 5. They were taken from the TSI DMA manual (which were taken from Wiedensohler 1988, Baron and Willeke 2005). The following equation was used for -2, -1, 0, 1, 2 charges (valid for 20 – 1000 nm):

$$\log f_i = \sum_{j=0}^5 a_j(N)(\log d)^j \quad (\text{Eq. 13})$$

Where d the particle diameter in nm and a_j are given in Table 4.

Table 4: Coefficients for Eq. 5 (estimation for number of elementary charge units).

$a_i(N)$	N=-2	N=-1	N=0	N=1	N=2
a_0	-26.3328	-2.3197	-0.0003	-2.3484	-44.4756
a_1	35.9044	0.6175	-0.1014	0.6044	79.3772
a_2	-21.4608	0.6201	0.3073	0.4800	-62.8900
a_3	7.0867	-0.1105	-0.3372	0.0013	26.4492
a_4	-1.3088	-0.1260	0.1023	-0.1553	-5.7480
a_5	0.1051	0.0297	-0.0105	0.0320	0.5049

2.5 Safety precautions

Generating aerosol can create a respiratory health hazard. Even if the excess from the generator is vented, there are times when the apparatus is open, or when tubes are disconnected and connected. For this reason care should be given in the choice of aerosol materials.

Another hazard is associated with the use of radioactive sources to “neutralise” the electrical charges on aerosols resulting from the generation process. A qualified physicist checked the radiation levels to evaluate the adequacy of the shielding, which was found adequate.

Finally the excess flow of the PNCs (which contains butanol) was also vented outside the building.

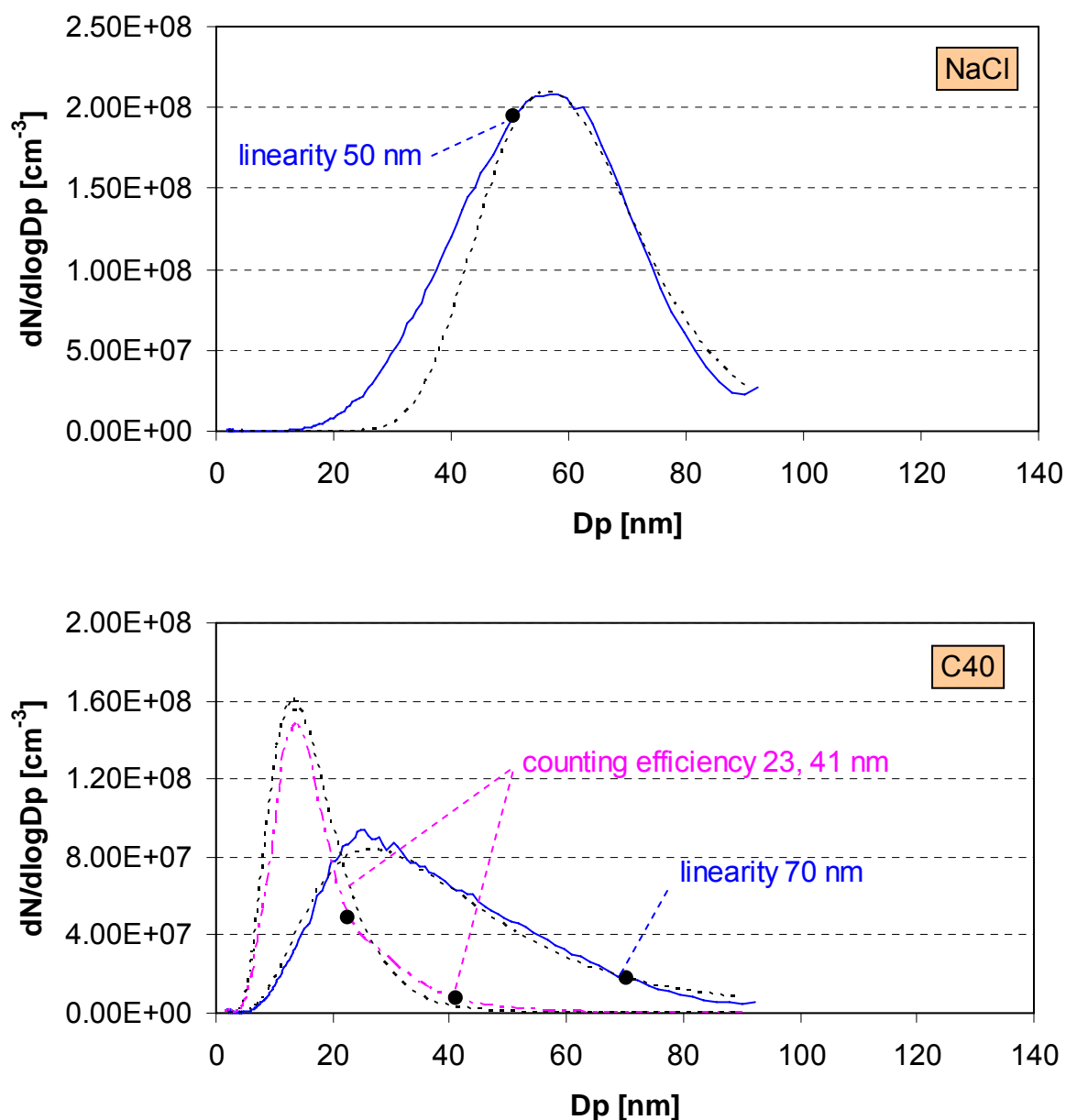
Table 5: Midpoint Mobilities, Midpoint Particle Diameters, and Fraction of Total Particle Concentration that Carries +1, +2, +3, +4, +5, and +6 Elementary Charges as a Function of Mobility.

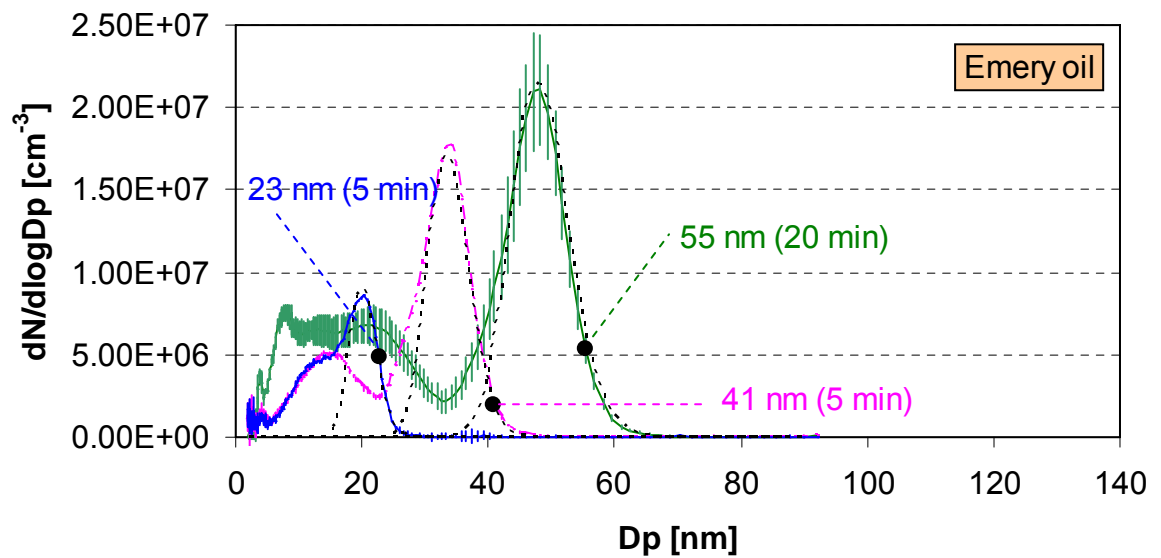
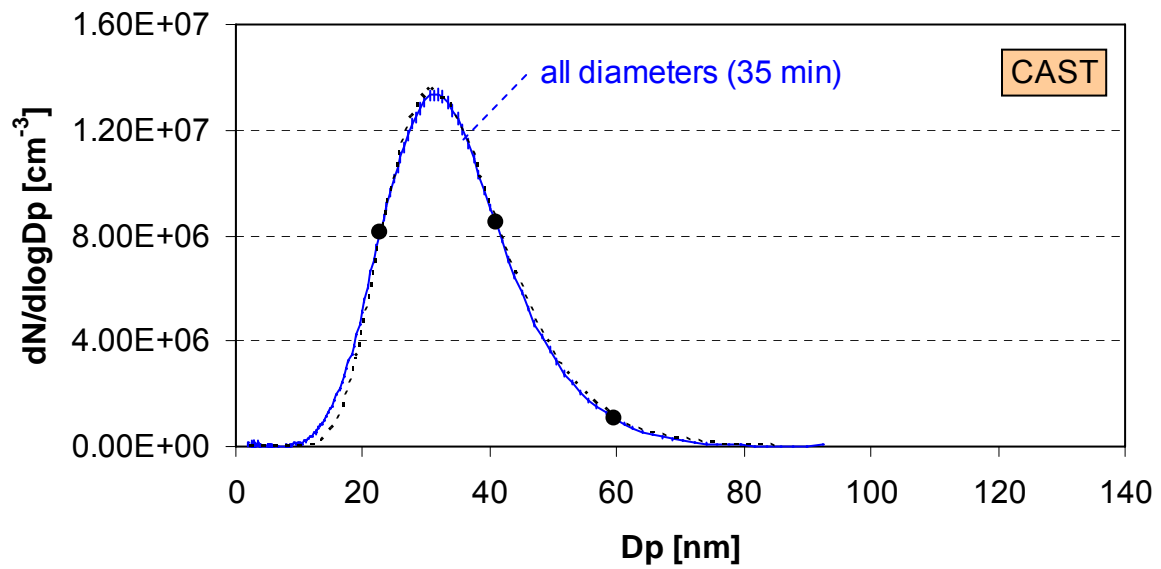
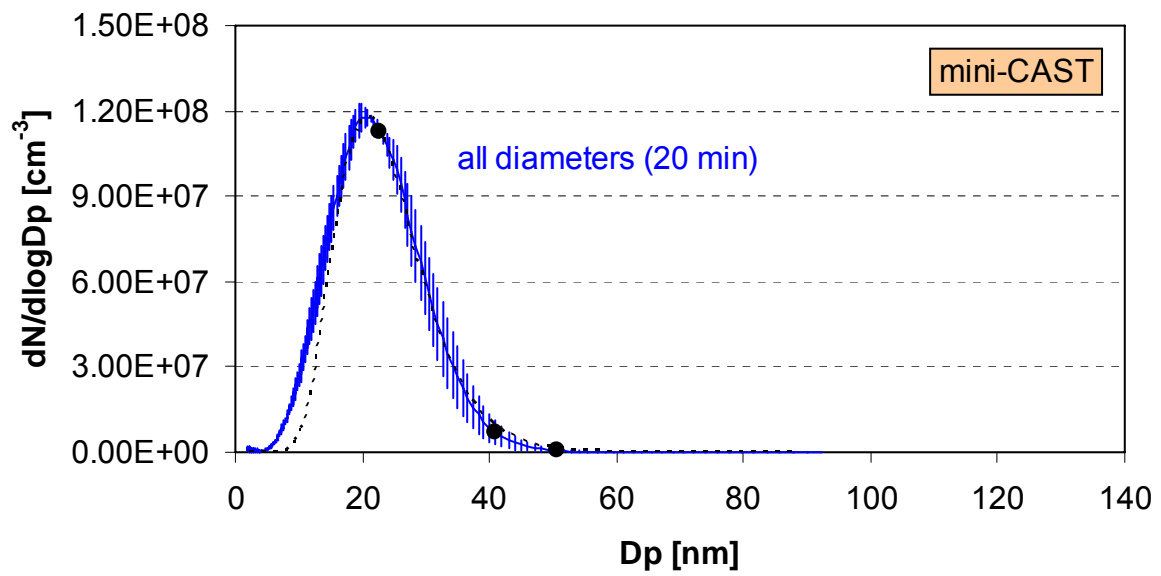
Mobility Midpoint cm ² /v-s	Particle Diameter Midpoint, μm	Fraction of Total Particle Concentration That Carries This Number (1-6) of Positive Charges					
		+1	+2	+3	+4	+5	+6
4.322E-1	0.0022	0.0082	0	0	0	0	0
3.243E-1	0.0025	0.0094	0	0	0	0	0
2.434E-1	0.0029	0.0108	0	0	0	0	0
1.827E-1	0.0034	0.0125	0	0	0	0	0
1.371E-1	0.0039	0.0146	0	0	0	0	0
1.030E-1	0.0045	0.0170	0	0	0	0	0
7.733E-2	0.0052	0.0199	0	0	0	0	0
5.808E-2	0.0060	0.0234	0	0	0	0	0
4.364E-2	0.0070	0.0275	0	0	0	0	0
3.280E-2	0.0081	0.0323	0	0	0	0	0
2.466E-2	0.0093	0.0380	0	0	0	0	0
1.855E-2	0.0107	0.0445	0	0	0	0	0
1.396E-2	0.0124	0.0520	0	0	0	0	0
1.051E-2	0.0143	0.0606	0	0	0	0	0
7.919E-3	0.0165	0.0703	0	0	0	0	0
5.972E-3	0.0191	0.0810	0	0	0	0	0
4.507E-3	0.0221	0.0928	0.0002	0	0	0	0
3.406E-3	0.0255	0.1054	0.0004	0	0	0	0
2.577E-3	0.0294	0.1188	0.0009	0	0	0	0
1.953E-3	0.0340	0.1327	0.0017	0	0	0	0
1.483E-3	0.0392	0.1467	0.0029	0	0	0	0
1.128E-3	0.0453	0.1605	0.0048	0	0	0	0
8.607E-4	0.0523	0.1737	0.0075	0	0	0	0
6.585E-4	0.0604	0.1857	0.0111	0	0	0	0
5.055E-4	0.0698	0.1963	0.0157	0	0	0	0
3.896E-4	0.0806	0.2050	0.0213	0.0006	0	0	0
3.016E-4	0.0931	0.2115	0.0280	0.0012	0	0	0
2.347E-4	0.1075	0.2155	0.0356	0.0024	0.0001	0	0
1.837E-4	0.1241	0.2169	0.0439	0.0041	0.0001	0	0
1.446E-4	0.1433	0.2158	0.0525	0.0067	0.0004	0	0
1.147E-4	0.1655	0.2122	0.0612	0.0100	0.0008	0	0
9.153E-5	0.1911	0.2065	0.0694	0.0140	0.0015	0.0001	0
7.360E-5	0.2207	0.1989	0.0768	0.0187	0.0027	0.0002	0
5.961E-5	0.2548	0.1898	0.0829	0.0236	0.0044	0.0005	0
4.862E-5	0.2943	0.1797	0.0873	0.0286	0.0065	0.0010	0.0001
3.993E-5	0.3398	0.1690	0.0901	0.0335	0.0091	0.0018	0.0002
3.299E-5	0.3924	0.1581	0.0910	0.0380	0.0121	0.0029	0.0005
2.742E-5	0.4532	0.1474	0.0903	0.0418	0.0153	0.0043	0.0010
2.290E-5	0.5233	0.1372	0.0883	0.0450	0.0185	0.0061	0.0016
1.921E-5	0.6043	0.1278	0.0854	0.0475	0.0215	0.0081	0.0025
1.618E-5	0.6978	0.1194	0.0821	0.0491	0.0243	0.0102	0.0037
1.367E-5	0.8058	0.1121	0.0789	0.0500	0.0267	0.0124	0.0050
1.159E-5	0.9306	0.1063	0.0763	0.0501	0.0286	0.0145	0.0065

3. GRIMM RESULTS

3.1 Size distributions of particles with different generators

Figure 8 shows the size distributions that were measured upstream the DMA, before the selection of the appropriate diameter for calibration (mentioned in the figure). The concentration was adjusted according to the needs of the measurement by adjusting the dilution upstream the classifier. Error bars, if plotted, indicate the stability of the measurements expressed as the CoV of 2-3 scans for the duration given in the parenthesis. The dashed lines show the log fitted distributions (minimising the right part of the distribution). The log fitted distributions will only be used at the discussion section for the estimation of the multi-charge effect of various distributions.





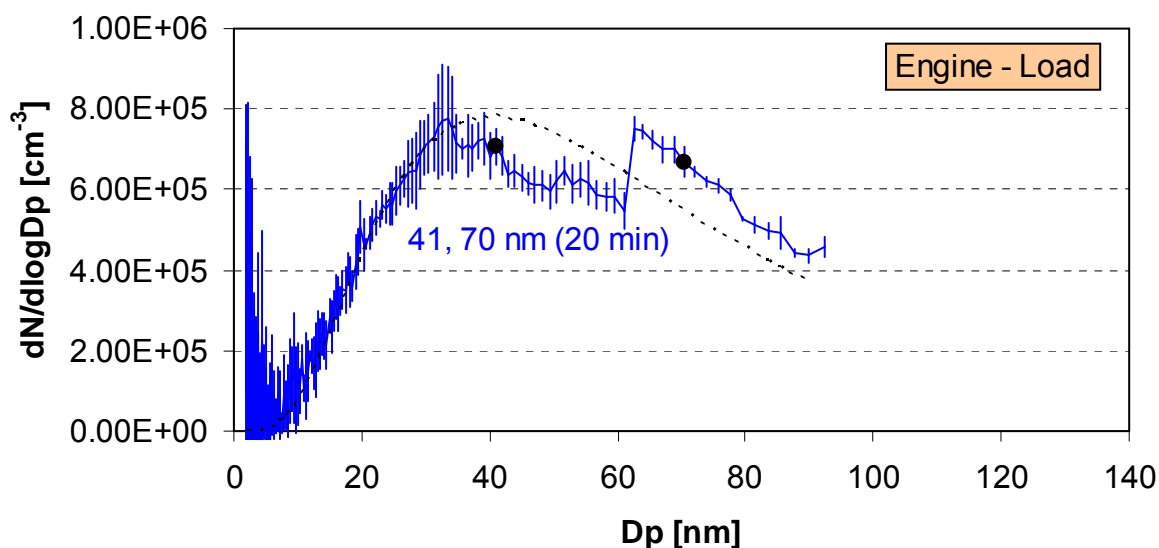


Figure 8: Particle size distributions entering the M-DMA.

Table 6: Characteristics of the size distributions of various materials.

Material	$N(\text{meas})$	$N(\text{fit})$	$D(m)$	σ	Diameter	ε	Stability
NaCl	6.60E+07	5.15E+07	55	1.28	50	15%	-
C40	6.00E+07	5.46E+07	13	1.60	23	-	-
	6.00E+07	5.46E+07	13	1.60	41	-	-
	5.02E+07	5.12E+07	26	1.73	70	1%	-
Engine load	1.27E+06	1.21E+06	39	1.91	41	-	7% (20 min)
	1.27E+06	1.21E+06	39	1.91	70	-	4% (20 min)
Mini CAST	1.07E+08	8.88E+07	20	1.35	23	0%	5% (20 min)
	1.07E+08	8.88E+07	20	1.35	41	-	58% (20 min)
	1.07E+08	8.88E+07	20	1.35	50	-	77% (20 min)
CAST	1.04E+07	9.87E+06	30.5	1.34	23	-	7% (35 min)
	1.04E+07	9.87E+06	30.5	1.34	41	-	9% (35 min)
	1.04E+07	9.87E+06	30.5	1.34	60	2.3%	25% (35 min)
Emery oil	7.06E+06	2.35E+06	19.7	1.11	23	-	2% (5 min)
	1.10E+07	3.99E+06	33.3	1.11	41	-	12% (5 min)
	1.84E+07	4.98E+06	47.2	1.10	55	0%	15% (20 min)

Table 6 summarises the characteristics of the size distributions shown in Figure 8. The measured size distributions were log fitted by minimising the error of the right hand part of the size distribution (e.g. after the peak). The parameters of the fitting are given in Table 6. The multi-charge effect ϵ was estimated by the equations given in the experimental section “Multi-charge effect”. Stability in this table is defined as the CoV of 2-3 scans for the duration given in parenthesis at the specific diameter +/-5 nm (see also Figure 8).

3.2 Primary method

With the primary method the PNCs under calibration are compared with the FCE.

Linearity

The linearity calibration requires the comparison of the PNC under calibration with an electrometer using at least six concentrations (including 0). The following tables give the gradient (slope) and the square of the Pearson product moment correlation coefficient (R²) of the comparison of the electrometer with the PNC under calibration, by forcing through the origin (zero concentration on both instruments). In addition, the differences of the concentrations of the electrometer and the PNC under calibration are calculated for each concentration tested and their average (without the zero point) subtracted by 1 are also given in the following tables (and the CoV) for each PNC under evaluation. The results were not corrected for the PNCs flow rates (negligible effect) and the multiply charged particles effect.

PNC model 5.404 S/N: 412 had a slope ~0.91, PNC model 5.404 S/N: 608 ~0.93 and PNC model 5.403 S/N: 003 ~0.99 (Table 7-Table 9). The gradient seemed to be material independent for soot, C40, and Emery Oil. Linearity didn't seem to be impacted by the particle size as long as it was chosen to be to the right of the mode of the particle size distribution and multi-charge effect was low (<2.5%).

Table 7: PNC model 5.404 S/N: 412

<i>Material</i>	<i>Slope</i>	<i>R²</i>	<i>1 – Difference</i>	<i>±CoV</i>
NaCl	0.762	0.9999	0.763	2.7
C-40-1	0.894	0.9996	0.908	2.2
C-40-2	0.894	0.9977	0.920	3.8
CAST	0.906	0.9991	0.924	3.0
Mini-CAST	0.922	0.9995	0.915	5.1
Emery oil	0.921	0.9990	0.939	3.0
Engine load	0.741	0.9989	0.756	2.4

Table 8: PNC model 5.404 S/N: 608

<i>Material</i>	<i>Slope</i>	<i>R2</i>	<i>1 – Difference</i>	<i>±CoV</i>
NaCl	0.785	0.9997	0.776	1.2
C-40-1	0.913	0.9999	0.926	3.7
C-40-2	0.921	0.9996	0.931	1.4
CAST	0.919	0.9997	0.921	1.6
Mini-CAST	0.936	0.9998	0.924	2.3
Emery oil	0.954	0.9999	0.955	0.7
Engine load	0.731	0.9996	0.739	1.7

Table 9: PNC model 5.403 S/N: 003 (Reference)

<i>Material</i>	<i>Slope</i>	<i>R2</i>	<i>1 – Difference</i>	<i>±CoV</i>
NaCl	0.854	0.9994	0.847	2.8
C-40-1	0.960	0.9992	0.949	2.9
C-40-2	0.991	0.9991	0.979	1.8
CAST	0.951	0.9999	0.956	1.0
Mini-CAST	0.986	0.9992	0.979	1.8
Emery oil	1.007	0.9986	0.987	2.8
Engine load	0.730	0.9980	0.747	2.9

The gradient for NaCl was considerably less. This was due to the fact that the size of the particles that were provided was rather large, the distribution was rather wide, so a considerable amount of multi-charge effect (estimated 15%) existed. In addition, NaCl particles do not reach their maximum efficiency at 50 nm but at higher diameters for PNCs with cut-off sizes at 23 nm (Wang et al. 2007). The particle size distribution for the particles from the engine was also very wide so that a lot of larger particles existed. All PNCs showed excellent linearity with R2 greater than 0.998 (0.97 required) for all materials in the concentration range 1000 to 10000 cm⁻¹.

The difference between the electrometer and the PNCs was generally <10% with the exception of NaCl and engine cases. The most important is that the CoV of difference was <3% indicating that the response of the counters is linear. Finally it should be mentioned that the slope and the 1-Difference have similar values.

Counting efficiency

The counting efficiency tests of the primary method are based on the comparison of the PNCs under calibration with the electrometer FCE (Table 10-Table 12). Figure 9-Figure 11 summarise the counting efficiency and linearity results for the three PNCs.

Table 10: PNC model 5.404 S/N: 412

<i>Material</i>	<i>23 nm</i>	<i>CoV</i>	<i>41 nm</i>	<i>CoV</i>
C-40-1	82.6	5.6	96.7	13.4
C-40-2	81.7	16.5	94.9	21.3
CAST	64.9	6.6	91.6	3.0
Mini-CAST	57.4	5.1	86.7	3.4
Emery oil	72.9	6.0	94.7	2.9
Engine load	-	-	82.3	8.2

Table 11: PNC model 5.404 S/N: 608

<i>Material</i>	<i>23 nm</i>	<i>CoV</i>	<i>41 nm</i>	<i>CoV</i>
C-40-1	81.0	5.7	93.5	13.6
C-40-2	80.9	17.0	93.8	21.8
CAST	59.9	6.9	91.1	2.8
Mini-CAST	56.0	5.1	86.5	3.4
Emery oil	72.6	5.9	95.4	3.1
Engine load	-	-	80.6	8.2

Table 12: PNC model 5.403 S/N: 003 (Reference)

<i>Material</i>	<i>23 nm</i>	<i>CoV</i>	<i>41 nm</i>	<i>CoV</i>
C-40-1	94.6	5.6	96.5	13.4
C-40-2	91.1	14.4	94.8	21.6
CAST	96.8	6.3	96.4	2.8
Mini-CAST	90.5	4.2	94.6	3.3
Emery oil	95.2	5.6	97.6	3.1
Engine load			85.3	8.5

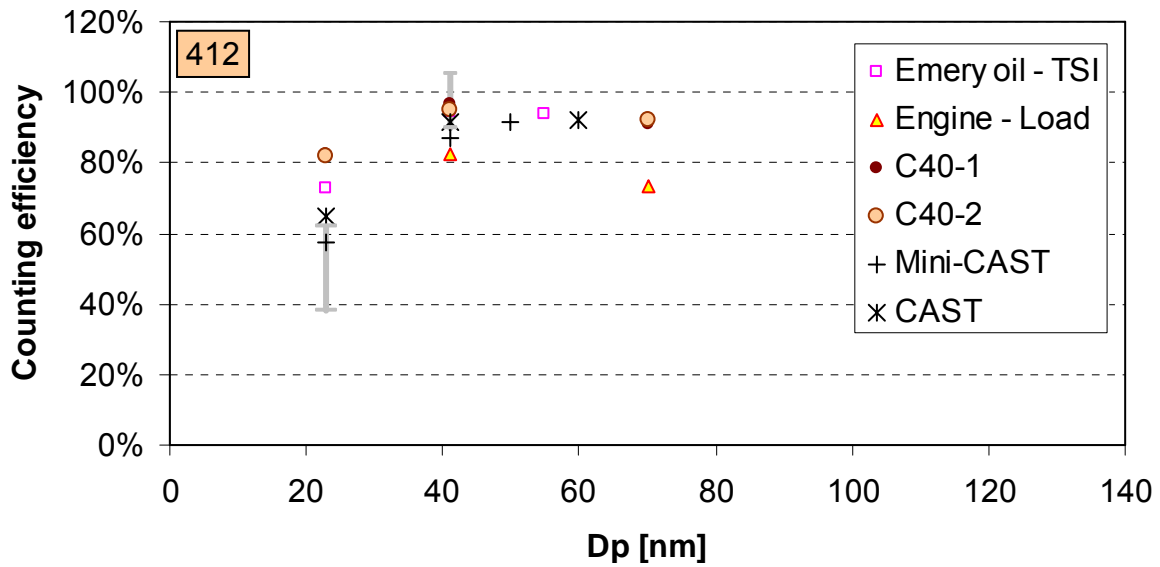


Figure 9: Counting efficiency of PNC model 5.404 S/N: 412

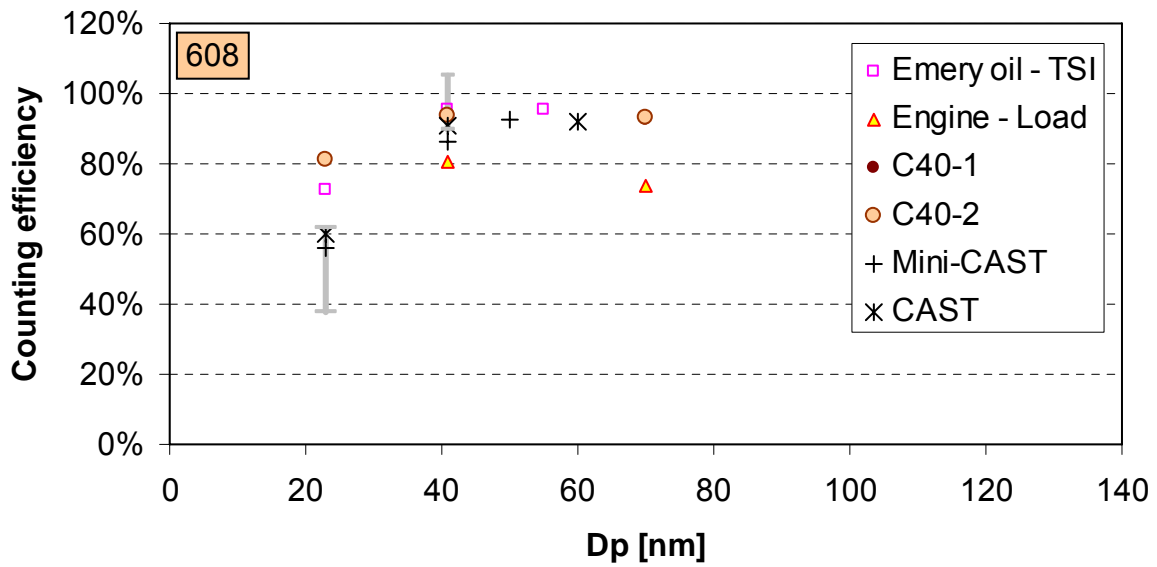


Figure 10: Counting efficiency of PNC model 5.404 S/N: 608

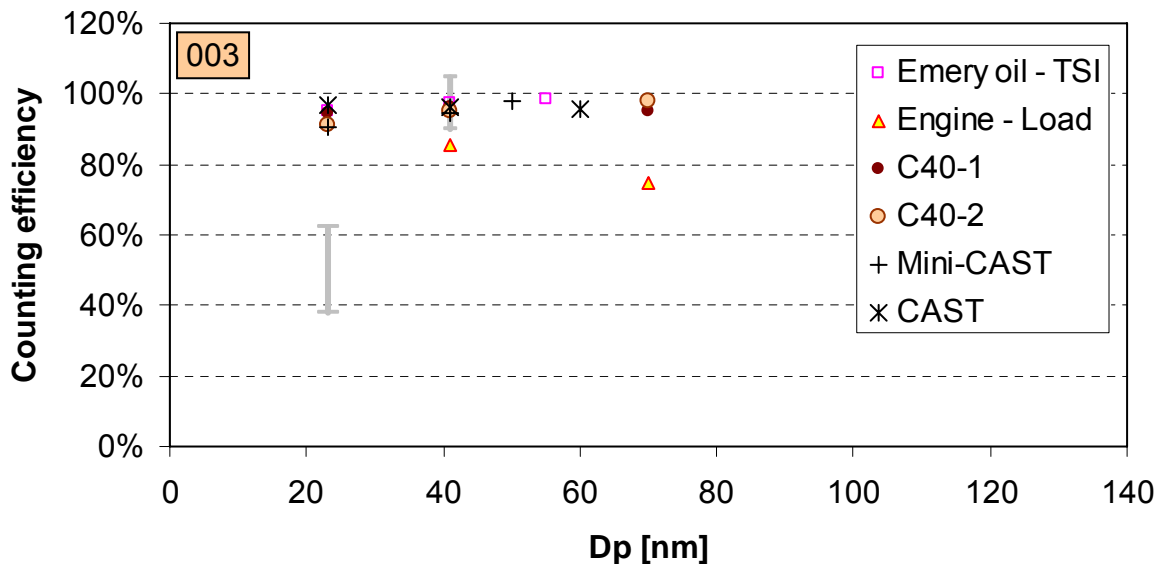


Figure 11: Counting efficiency of PNC model 5.403 S/N: 003 (Reference).

Generally C40 particles showed higher counting efficiency than the rest materials. The CAST particles were found within the $50\pm 12\%$ PMP limits for the PMP PNCs (412 and 608). For the JRC engine no value at 23 nm could be measured due to the limited runtime of the engine. The counting efficiency with engine particles at 41 nm turned out to be about 5% lower than for the other particle generators.

In general the counting efficiency of the PNC 412 and 608 at 23 nm was found at the high end of the PMP requirements ($50\pm 12\%$) for all materials because they were calibrated with NaCl. In general the counting efficiency of the two PNCs at 41 nm was $\geq 90\%$ (without any multi-charge correction).

3.3 Secondary method

According to the secondary method, the PNCs under evaluation are compared with a calibrated PNC. In the GRIMM case the reference PNC was PNC model 5.403 S/N: 003 (with $d_{50} < 10$ nm). No correction was applied to the Reference PNC at the following results. This correction should be ~ 0.99 (see Table 9) depending on the material of the primary calibration of the specific PNC.

Linearity

The secondary linearity method showed that PNC 412 had a slope ~ 0.93 and PNC 608 ~ 0.95 (Table 13-Table 14). The gradient seemed to be material independent for soot, C40, and Emery Oil. The gradient for NaCl was slightly less ($< 5\%$). The secondary method is less sensitive to the multi charge effect compared to the primary method ($< 15\%$). However there is still an effect (see Experimental methods, paragraph “multi charge effect”). Both GRIMM PNCs 412 and 608 when compared to the reference PNC 003 showed excellent linearity with R^2 greater than 0.994 and 0.997 (0.97 required) respectively for all materials in the concentration range 1000 to 10000 cm^{-1} .

The difference between the PNCs was generally $< 10\%$. The most important is that the CoV of difference was $< 5\%$ indicating that the response of the counters was linear. Finally it should be mentioned that the slope and the 1-Difference had similar values.

Table 13: PNC model 5.404 S/N: 412

<i>Material</i>	<i>Slope</i>	<i>R2</i>	<i>Difference</i>	\pm CoV
NaCl	0.892	0.9991	0.902	5.1
C-40-1	0.931	0.9976	0.958	4.9
C-40-2	0.902	0.9940	0.941	5.1
CAST	0.953	0.9991	0.970	2.6
Mini-CAST	0.935	0.9977	0.935	6.5
Emery oil	0.914	0.9954	0.952	5.7
Engine load	1.015	0.9998	1.011	0.7

Table 14: PNC model 5.404 S/N: 608

<i>Material</i>	<i>Slope</i>	<i>R2</i>	<i>Difference</i>	<i>±CoV</i>
NaCl	0.919	0.9999	0.918	1.9
C-40-1	0.951	0.9994	0.975	2.8
C-40-2	0.930	0.9976	0.951	2.9
CAST	0.960	0.9996	0.967	1.2
Mini-CAST	0.950	0.9998	0.943	3.3
Emery oil	0.947	0.9985	0.968	3.0
Engine load	1.000	0.9992	0.989	1.7

Counting Efficiency

The counting efficiency according to the secondary method was checked by comparing the concentrations of the PNCs under calibration with the reference PNC (at various diameters). The counting efficiency of the reference PNC at the particular diameters should be taken into account. In the results presented below the counting efficiency of the Reference PNC 003 was considered 1 at 23 and 41 nm. No correction was applied for the slope (see Table 9, a correction ~0.99 should be applied depending on the material).

In general the counting efficiency of PNC 412 and 608 at 23 nm was higher than 50% for all materials as the original calibration was with NaCl particles. The counting efficiency of the two PNCs at 41 nm was >=90%. Figure 12-Figure 13 summarise the counting efficiency and linearity results for the two PNCs.

Table 15: PNC model 5.404 S/N: 412

<i>Material</i>	<i>23 nm</i>	<i>CoV</i>	<i>41 nm</i>	<i>CoV</i>
C-40-1	87.3	5.4	100.2	11.9
C-40-2	89.6	14.5	100.1	19.6
CAST	67.0	4.1	95.0	2.3
Mini-CAST	63.5	4.0	91.7	2.5
Emery oil	76.6	3.1	97.0	2.5
Engine load	-	-	96.5	4.7

Table 16: PNC model 5.404 S/N: 608

Material	23 nm	CoV	41 nm	CoV
C-40-1	86.7	5.5	97.0	12.2
C-40-2	88.8	15.1	98.9	20.0
CAST	61.8	4.4	94.5	2.2
Mini-CAST	61.9	3.9	91.5	2.5
Emery oil	76.2	2.9	97.7	2.7
Engine load	-	-	94.4	4.7

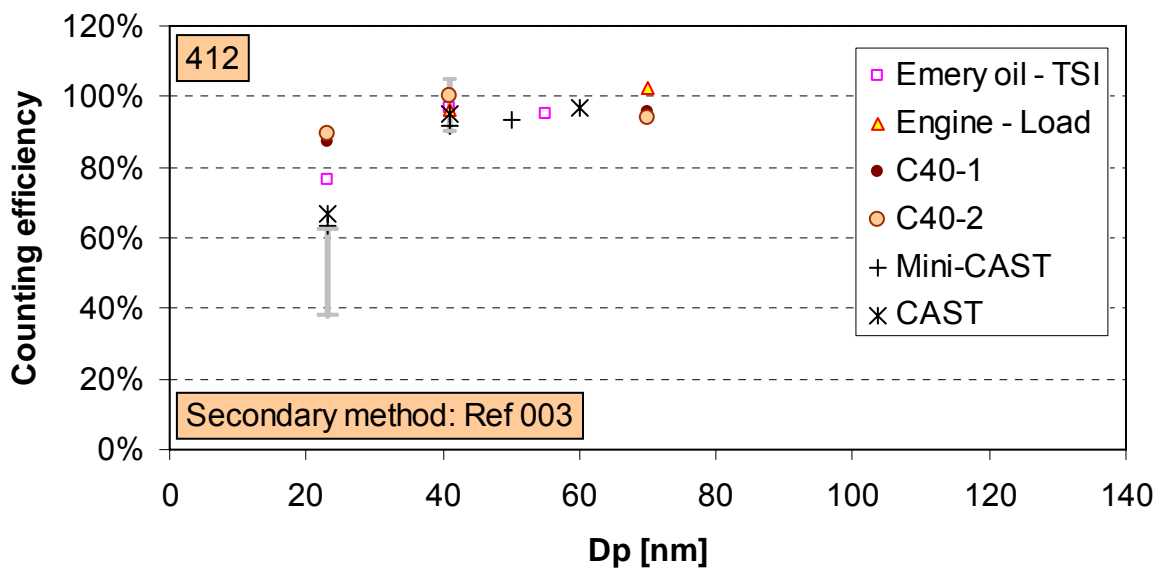


Figure 12: Counting efficiency of PNC 412 according to the secondary method.

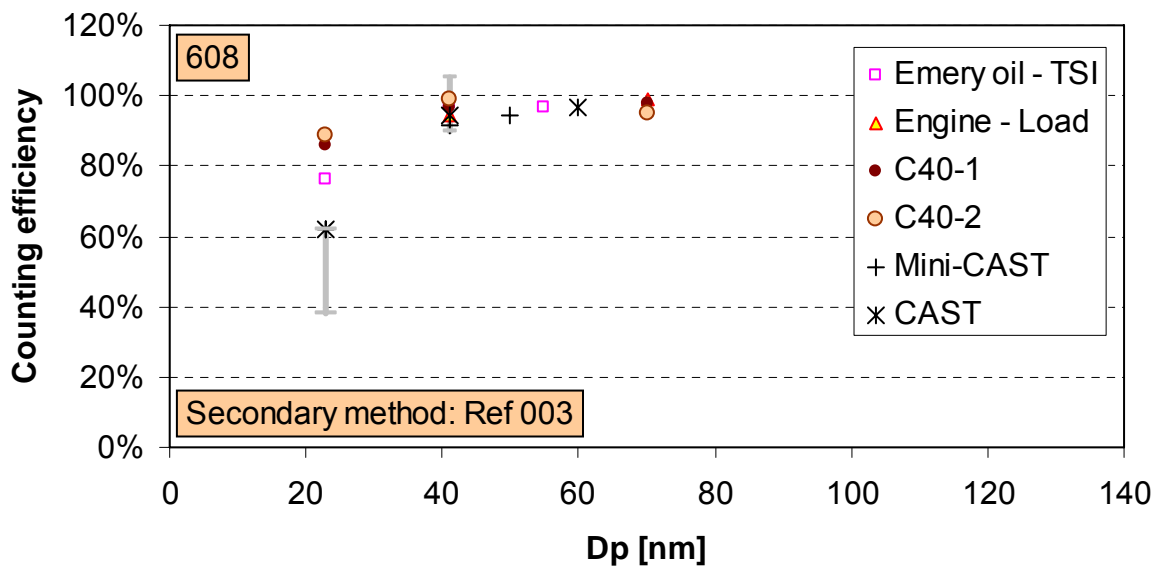


Figure 13: Counting efficiency of PNC 608 according to the secondary method.

Comparison of primary and secondary methods

Comparing the results for PNC 412 and 608 of the primary and secondary method the following are observed:

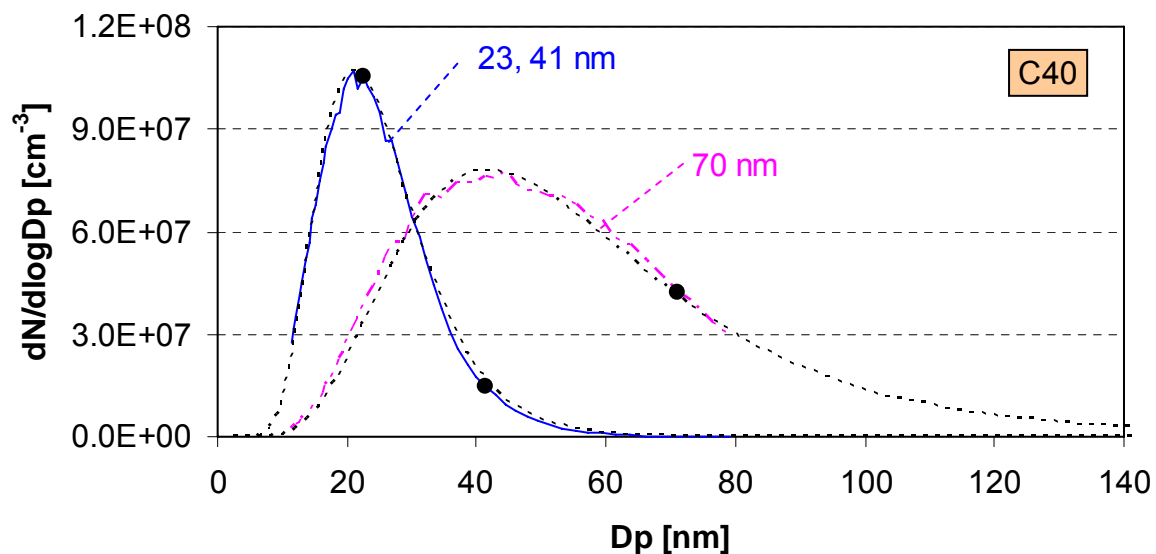
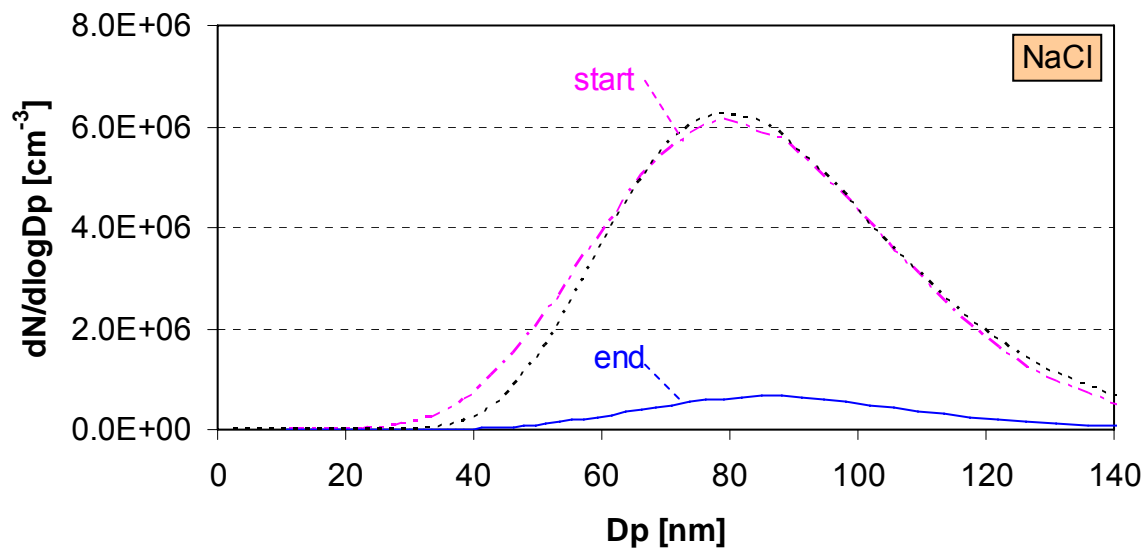
- The slopes with the secondary method were slightly higher (~2%), but if the slope of the reference PNC 033 was taken into account then there would be no difference.
- The counting efficiencies at 23 nm with the secondary method were around 5% higher. This had to do with the 95% efficiency of the reference PNC at this diameter. This correction should be taken into account for accurate results.
- The counting efficiencies at 41 nm with the secondary method were around 3% higher. This had to do with the 97% efficiency of the reference PNC at this diameter. This correction should be taken into account for accurate results.

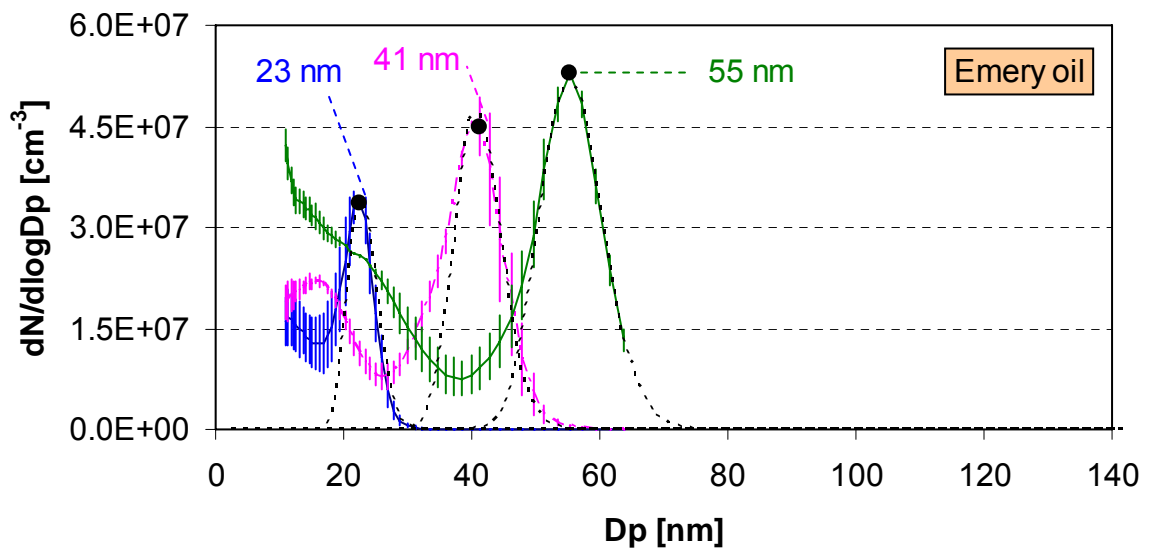
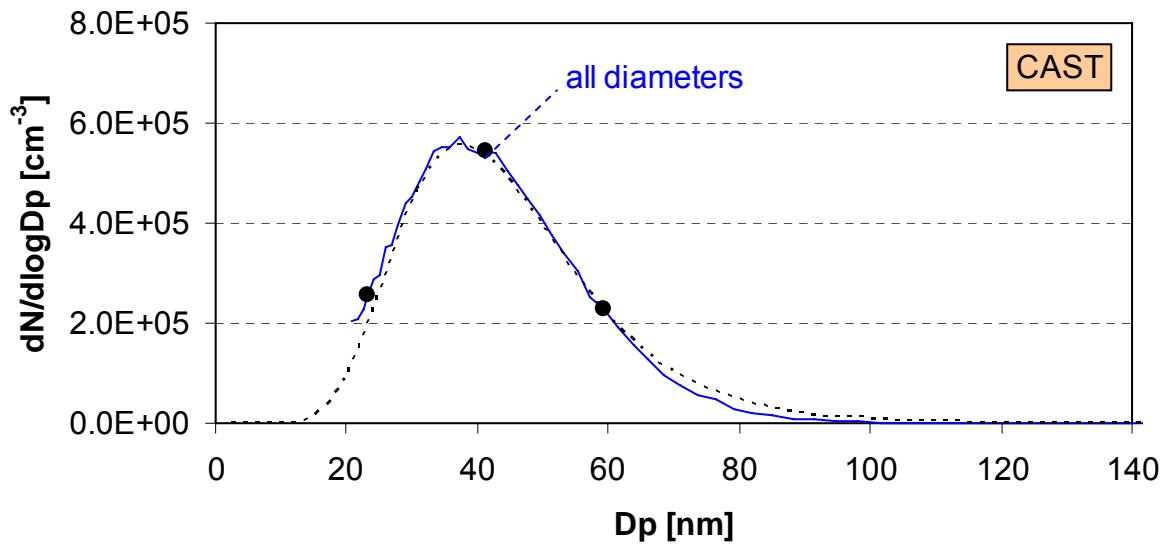
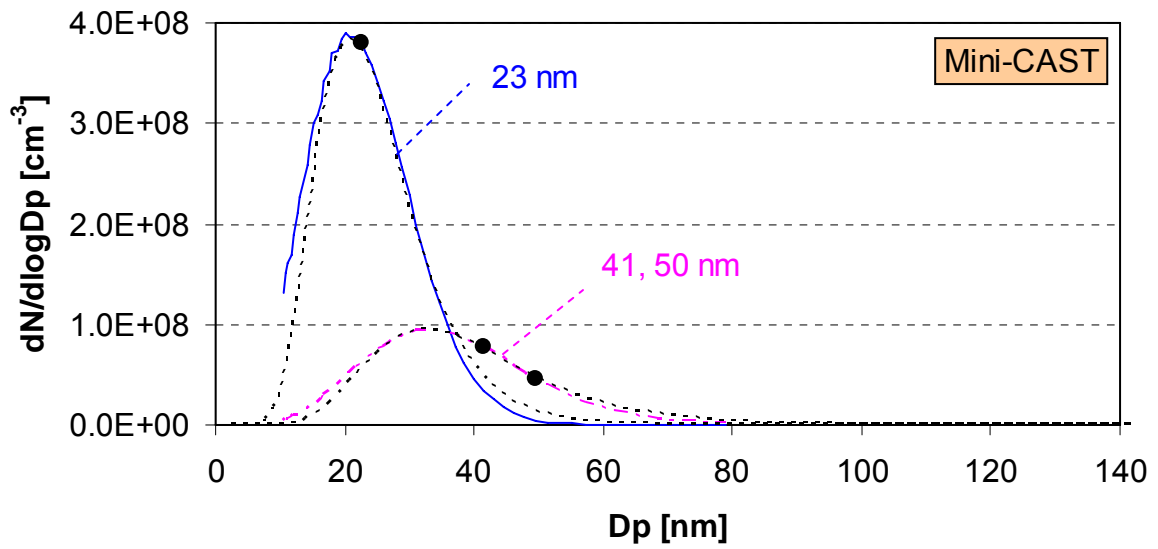
Summarising, the primary and the secondary methods are equivalent as long as the correct coefficients of the reference PNC are taken into account.

4. TSI RESULTS

4.1 Size distributions of particles with different generators

Figure 14 shows the size distributions that were measured upstream the DMA, before the selection of the appropriate diameter. The concentration was adjusted according to the needs of the measurement by adjusting the dilution upstream the classifier. Error bars for the engine case indicate the stability of the measurements expressed as the CoV of 2-3 scans for the duration given in the parenthesis. Error bars for emery oil indicate the repeatability of two days measurements (expressed as the CoV of 2 scans). The dashed lines show the log fitted size distributions (for the discussions in section 5). Figure 15 shows the engine size distributions during the extra tests that were conducted from TSI.





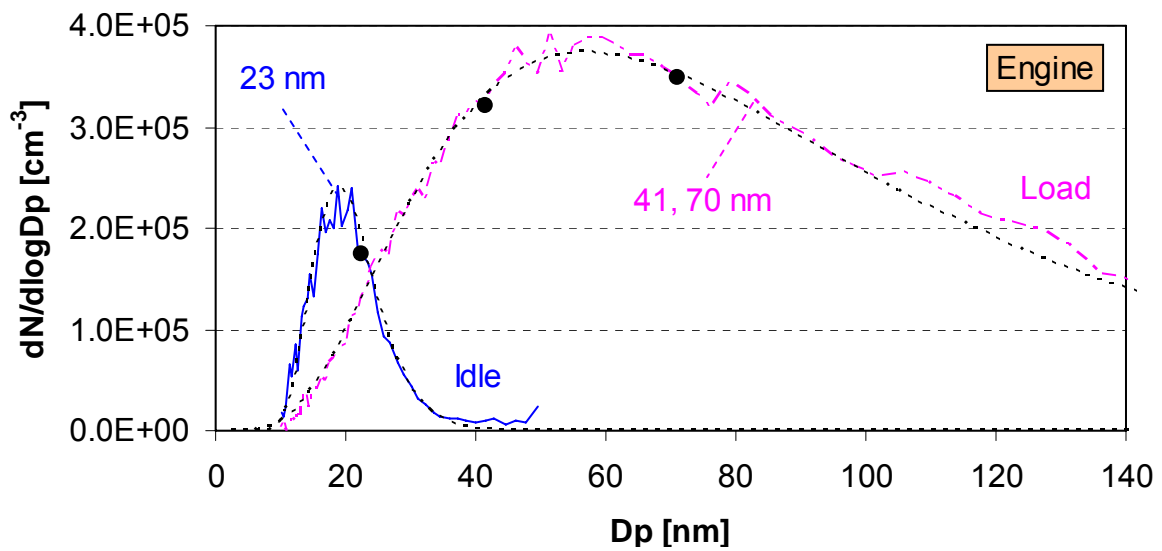


Figure 14: Particle size distributions entering the nano-DMA.

Extra engine tests

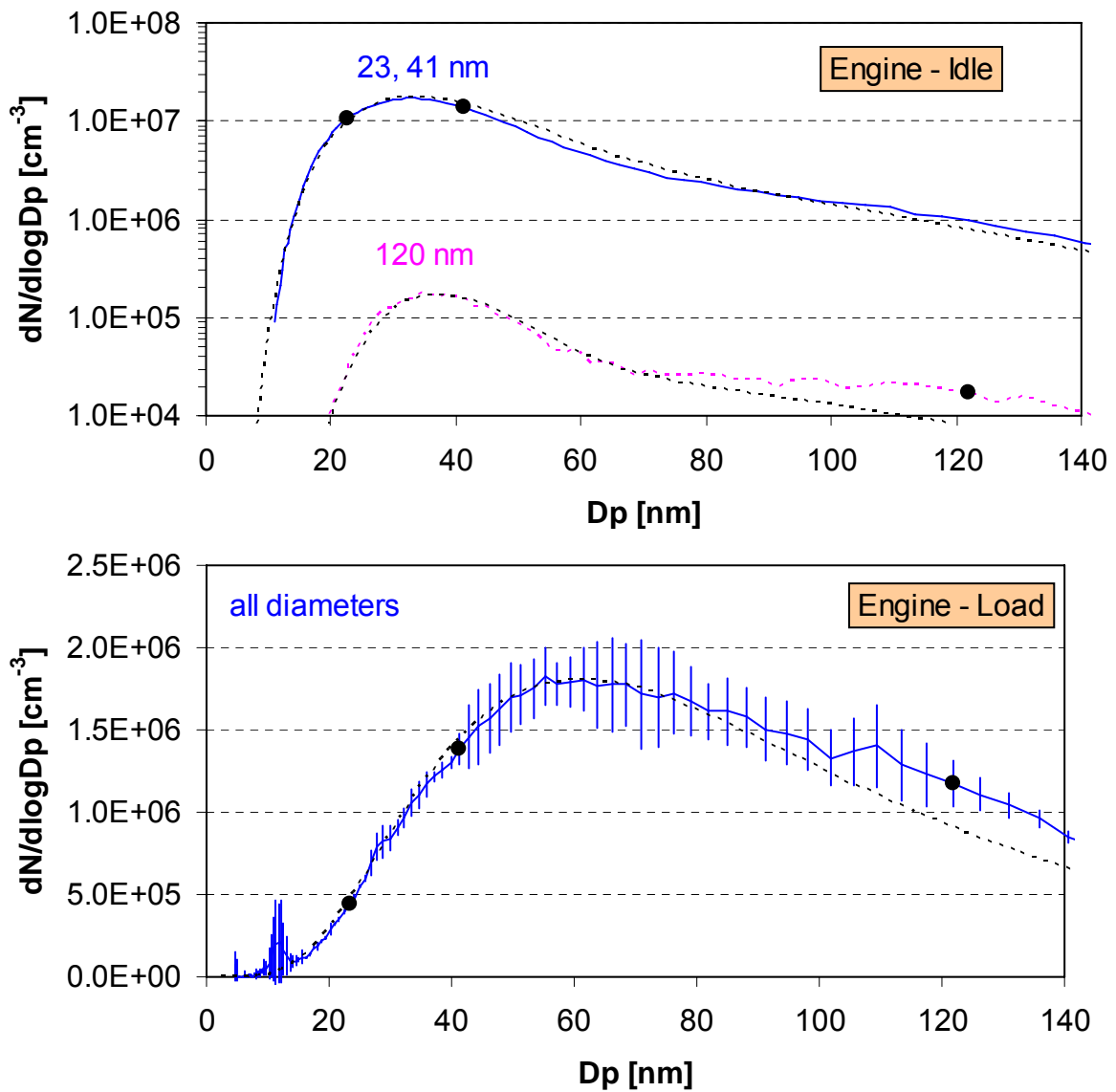


Figure 15: Particle size distributions entering the nano-DMA.

Table 17: Characteristics of the size distributions of various materials.

<i>Material</i>	<i>N(meas)</i>	<i>N(fit)</i>	<i>D(m)</i>	σ	<i>Diameter</i>	ε	<i>Stability</i>
NaCl	-	-	-	-	23		
	-	-	-	-	41		
	1.94E+06	1.84E+06	78.0	1.31	80	6.16%	
C40	3.91E+07	4.10E+07	20.7	1.42	23	0.24%	
	3.91E+07	4.10E+07	20.7	1.42	41	0.14%	
	3.81E+07	3.99E+07	41	1.60	70	3.45%	
Mini CAST	1.53E+08	1.41E+08	20.5	1.40	23	1.59%	
	3.91E+07	3.71E+07	32	1.43	41	0.09%	
	3.91E+07	3.71E+07	32	1.43	50	0.97%	
CAST	2.04E+05	2.04E+05	37	1.40	23	2.27%	
	2.04E+05	2.04E+05	37	1.40	41	2.29%	
	2.04E+05	2.04E+05	37	1.40	60	0.44%	
Emery	7.36E+06	3.61E+06	22.3	1.10	23	0.01%	25%**
	1.32E+07	4.50E+06	40.0	1.09	41	0.01%	14%**
	1.98E+07	4.95E+06	54.2	1.09	55	0.01%	8%**
Eng. Idle*	6.60E+04	6.60E+04	18.5	1.28	23		
Eng. Load	2.49E+05	2.47E+05	56	1.90	41		
Eng. Load	2.49E+05	2.47E+05	56	1.90	70		
Eng. idle*	7.20E+06	6.40E+06	32	1.42	23	11.0%	
	5.63E+04	4.31E+04	36	1.28	41	4.6%	
	5.63E+04	4.31E+04	36	1.28	120	3.18%	
Eng. load	1.16E+06	1.10E+06	60	1.80	23	3.66%	5%
	1.16E+06	1.10E+06	60	1.80	41	8.55%	9%
	1.16E+06	1.10E+06	60	1.80	120	8.97%	10%

* Both NM and AM

** Repeatability of 2 different days

Table 17 summarises the characteristics of the size distributions shown in Figure 14 and Figure 15. The measured size distributions were log fitted by minimising the error of the right hand part of the size distribution (e.g. after the peak). The parameters of the fitting are given in Table 17. The multi-charge effect was estimated by the equations given in the experimental section “Multi-charge effect”. Stability (for engine) in this table is defined as the CoV of 2-3 scans for the duration given in parenthesis at the specific diameter +/-5 nm (see also Figure 8). For the emery oil the repeatability is given as the measurements were conducted on two different days.

4.2 Primary method

With the primary method the PNCs under calibration are compared with the AE.

Linearity

The linearity calibration requires the comparison of the PNC under calibration with an electrometer using at least six concentrations (including 0). The following tables give the gradient (slope) and the square of the Pearson product moment correlation coefficient (R²) of the comparison of the electrometer with the PNC under calibration, by forcing through the origin (zero concentration on both instruments). In addition, the differences of the concentrations of the electrometer and the PNC under calibration are calculated for each concentration tested and their average (without the zero point) subtracted by 1 are also given in the following tables (and the CoV) for each PNC under evaluation. The results in this section were not corrected for the PNC flowrates and any multiple charged particles effect.

The observations are:

- The JRC 3790 linearity slopes were generally higher than 0.92. However they were found only 0.83 for NaCl, 0.79-0.88 for the engine cases. These low values had to do with the high effect of the multiply charged particles as it will be explained in the discussion section.
- The 3010D and TSI 3790 slopes were found lower probably due to a non-uniform splitting among instruments. The flow uniformity was checked in the middle of the workshop (after NaCl, C40 and Mini-CAST experiments, but before the Matter CAST, engine and emery oil measurements). It was noticed that the TSI 3790 agreed better with the JRC 3790 after the concentration uniformity checks, but it agreed better with JRC 3010D before that. It was suspected that concentration non-uniformity played a role in this discrepancy. The tests of the 3010D seem also affected by this non-uniform splitting. For these reasons the counting efficiency results from TSI 3790 and 3010D will not be taken into account on the discussions.
- The TSI 3776 consistently had slopes close to one (since the electrometer reading was normalized with 3776 concentration). The 3776 will serve as a reference PNC for secondary calibration.
- The JRC 3025 consistently had slopes 1.1-1.15. Probably this had to do with the higher than nominal values of the total and/or internal aerosol flow rates. The aerosol flow couldn't be checked during the workshop because there was not a flow meter in that flow range available.

- The linearity of the 3790's, 3776 and 3025A did not highly depend on the aerosol material tested in the workshop. However, they were found lower for NaCl and engine particles due to the multi-charge effect. The out-of-calibration 3010D linearity slope had high material dependence probably because this PNC had a lower ΔT , which enhanced the material dependence (Wang et al. 2007).
- The results were not corrected for the PNCs flowrates (as it is desirable to include the flow rate effect in the slope). If the flow rate was taken into account (Table 2) there would be a small difference. E.g. for PNC 3790 JRC the results would be 1.2% higher ($1/0.988=1.012$).
- R2 values were higher than 0.997 (0.97 required) for all materials and PNCs. The slopes and the 1-Difference values were similar. The CoVs were generally below 5%.

Table 18: PNC JRC 3790

<i>Material</i>	<i>Slope</i>	<i>R2</i>	<i>1 – Difference</i>	\pm CoV
NaCl	0.894	0.9995	0.890	2.9
C-40	0.943	0.9999	0.949	1.3
CAST	0.926	0.9999	0.926	1.1
Mini-CAST	0.924	0.9981	0.953	5.8
Engine (load)	0.848	0.9997	0.843	1.9
Emery oil - TSI	0.973	1.0000	0.968	1.2
Emery oil -AIST	0.951	0.9998	0.961	1.7
Engine idle	0.784	0.9984	0.805	4.0
Engine load	0.885	0.9966	0.925	9.1

Table 19: PNC TSI 3790

<i>Material</i>	<i>Slope</i>	<i>R2</i>	<i>1 – Difference</i>	\pm CoV
NaCl	0.893	0.9996	0.889	2.9
C-40	0.919	0.9999	0.924	1.3
CAST	0.926	0.9998	0.928	1.0
Mini-CAST	0.799	0.9980	0.824	5.9
Emery oil - TSI	0.973	0.9998	0.980	1.1
Engine idle	0.776	0.9971	0.803	4.8

Table 20: PNC 3010D

<i>Material</i>	<i>Slope</i>	<i>R2</i>	<i>1 – Difference</i>	<i>±CoV</i>
NaCl	0.839	0.9996	0.827	3.8
C-40	0.939	0.9998	0.935	0.9
CAST	0.845	0.9991	0.832	2.3
Mini-CAST	0.796	0.9995	0.809	3.0
Engine (load)	0.726	0.9978	0.713	4.4

Table 21: PNC 3776

<i>Material</i>	<i>Slope</i>	<i>R2</i>	<i>1 – Difference</i>	<i>±CoV</i>
Emery oil - TSI	0.997	0.9999	0.991	1.3
Emery oil -AIST	1.003	1.0000	1.009	1.0
Engine load	0.906	0.9987	0.928	4.6

Table 22: PNC 3025A

<i>Material</i>	<i>Slope</i>	<i>R2</i>	<i>1 – Difference</i>	<i>±CoV</i>
Emery oil - TSI	1.114	0.9999	1.106	1.3
Emery oil -AIST	1.140	0.9997	1.150	1.7
Engine idle	0.900	0.9979	0.928	4.4
Engine load	1.042	0.9970	1.087	8.5

Counting efficiency

The counting efficiency tests of the primary method are based on the comparison of the PNCs under calibration with the electrometer AE. The results of the engine particles are reported but only those extra tests which were more reliable are plotted.

Table 23: PNC JRC 3790

<i>Material</i>	<i>23</i>	<i>CoV</i>	<i>41</i>	<i>CoV</i>
C-40	0.862	2.9	1.033	2.6
CAST	0.504	1.1	0.960	2.6
Mini-CAST	0.522	1.3	0.916	4.8
Engine (load)	0.660	11.0	0.522	16.0
Emery oil - TSI	0.724	0.9	0.984	1.9
Emery oil -AIST	0.532	0.8	0.947	1.8
Engine idle	0.835	4.4	0.941	1.9
Engine load	0.573	2.3	1.013	3.2

Table 24: PNC TSI 3790

<i>Material</i>	<i>23</i>	<i>CoV</i>	<i>41</i>	<i>CoV</i>
C-40	0.625	4.5	0.975	7.3
CAST	0.406	1.3	0.899	2.4
Mini-CAST	0.159	1.8	0.734	4.8
Engine (load)	0.472	14.0	0.483	16.0
Emery oil - TSI	0.727	0.9	0.957	1.8
Engine idle	0.873	4.1	0.918	1.8

Table 25: PNC 3010D

<i>Material</i>	<i>23</i>	<i>CoV</i>	<i>41</i>	<i>CoV</i>
C-40	0.577	4.1	0.907	7.0
CAST	0.045	28.2	0.589	2.9
Mini-CAST	0.142	6.5	0.685	5.3
Engine (load)	0.222	15.0	0.386	16.0

Table 26: PNC 3776

<i>Material</i>	23	CoV	41	CoV
Emery oil - TSI	1.003	1.3	0.995	2.4
Emery oil -AIST	0.979	1.0	1.011	1.6
Engine load	1.022	2.3	1.021	3.2

Table 27: PNC 3025A

<i>Material</i>	23 nm	CoV	41 nm	CoV
Emery oil - TSI	1.121	2.1	1.128	2.4
Emery oil -AIST	1.124	-	1.149	-
Engine idle	1.116	4.7	1.095	2.7
Engine load	1.129	4.1	1.168	3.9

The observations are:

- The JRC 3790 PNC meets PMP counting efficiency requirements for CAST and emery oils. However, the emery oil data taken with the TSI method had a higher efficiency (74.8%) than the PMP specification, probably due to electrometer drift. The AIST method, which takes longer, takes into account any drift and is highly recommended when there are no time restrictions. C40 had significantly higher counting efficiencies at 23 nm than the rest materials. The data of the engine at idle mode were difficult to explain. They had very high counting efficiency at 23 nm, but lower efficiency at 120 nm. High fractions of multiple-charged particles (see Table 17), and the nature of particles in the nucleation mode might have contributed to these phenomena. The uncertainty of the specific measurements was also high (30%, see 5.3.1).
- The TSI 3790 PNC met PMP counting efficiency requirements for C40 and Matter CAST. Other materials failed at either 23 nm or 41 nm.
- The JRC 3010D read lower concentrations than the 3790s. This instrument, as mentioned in the linearity results requires factory recalibration and service.
- The TSI 3776 had counting efficiencies ~100% over the range of 23-55 nm for emery oil (since the electrometer reading was normalized with 3776 concentration). Therefore it will serve as a reference for the secondary calibration procedure.
- The JRC 3025A read ~113% for emery oil, maybe due to internal flow error (in agreement with the linearity data). The engine exhaust results were difficult to explain. The counting efficiency of 3776 and 3025A were significantly higher than

unity at 23 nm and 41 nm (engine load). The exact reason is not clear. Possible reasons are new particle formation inside the CPC due to volatile vapor or electrometer drift. Limited data showed that the AE drifted more during diesel engine exhaust measurement than normal runs, which will be discussed later. There were significant amount of doubly charge particles.

- Accounting for experimental uncertainties, emery oil and CAST can meet PMP specifications. C40 gave higher efficiencies but still can be used. Idle engine had high uncertainties.

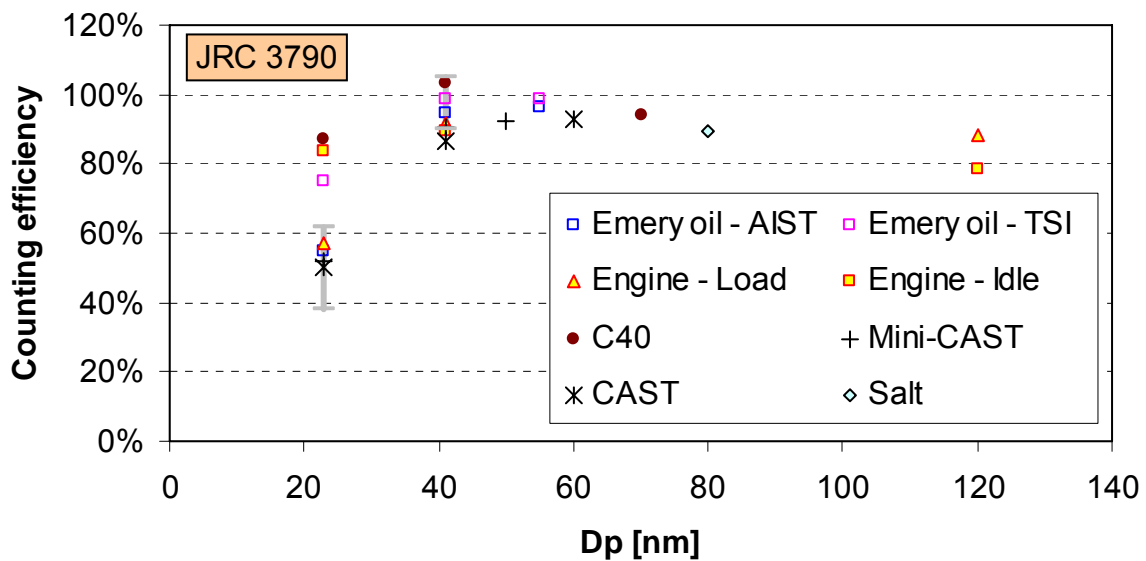


Figure 16: Counting efficiency of PNC JRC 3790 (without engine medium)

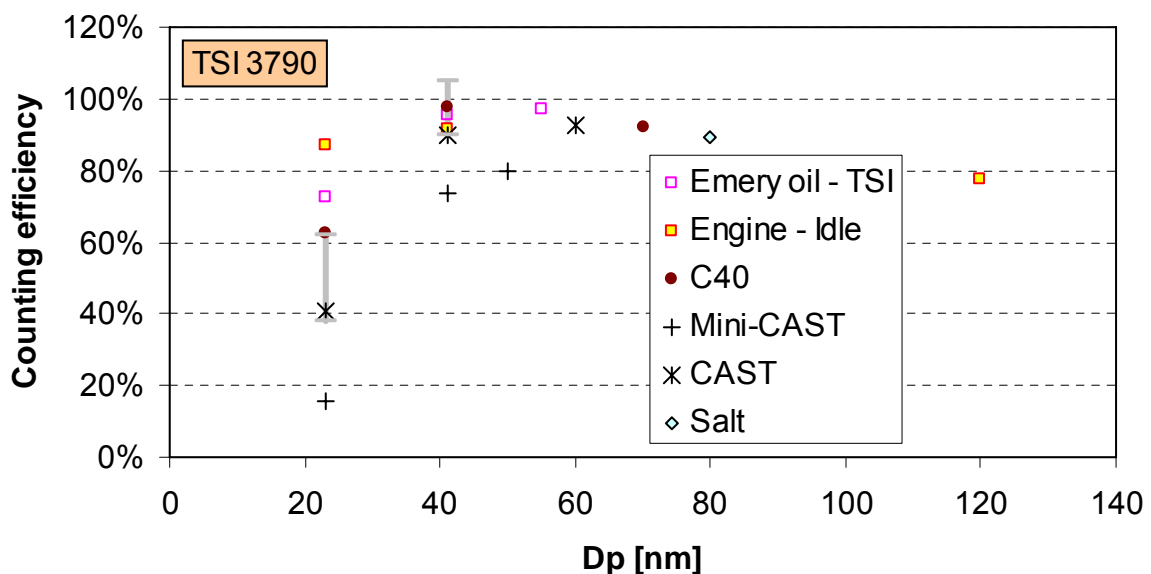


Figure 17: Counting efficiency of PNC TSI 3790

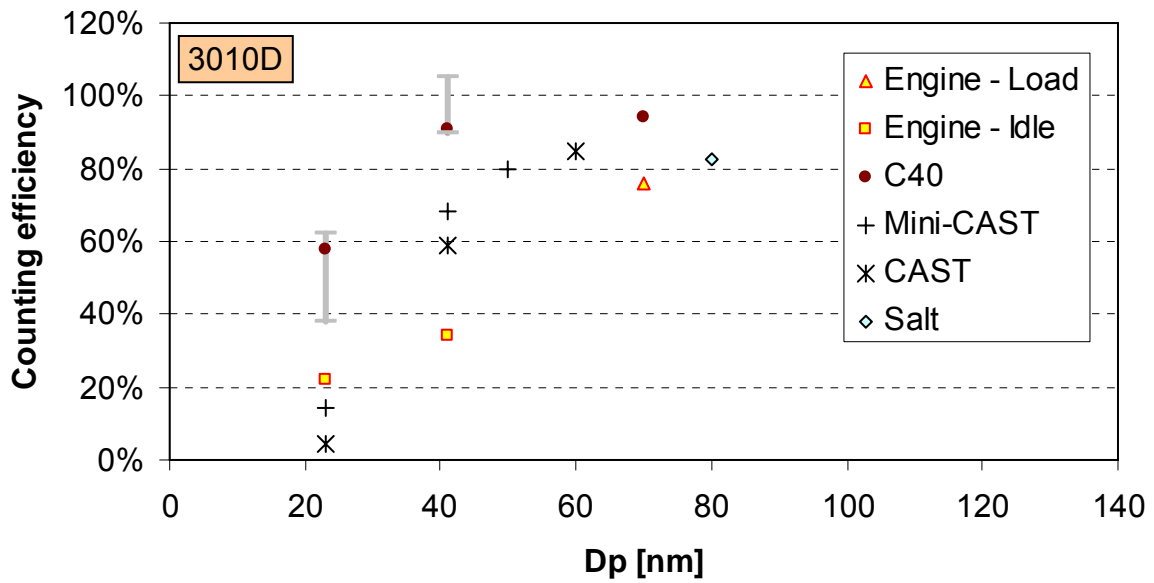


Figure 18: Counting efficiency of PNC 3010D

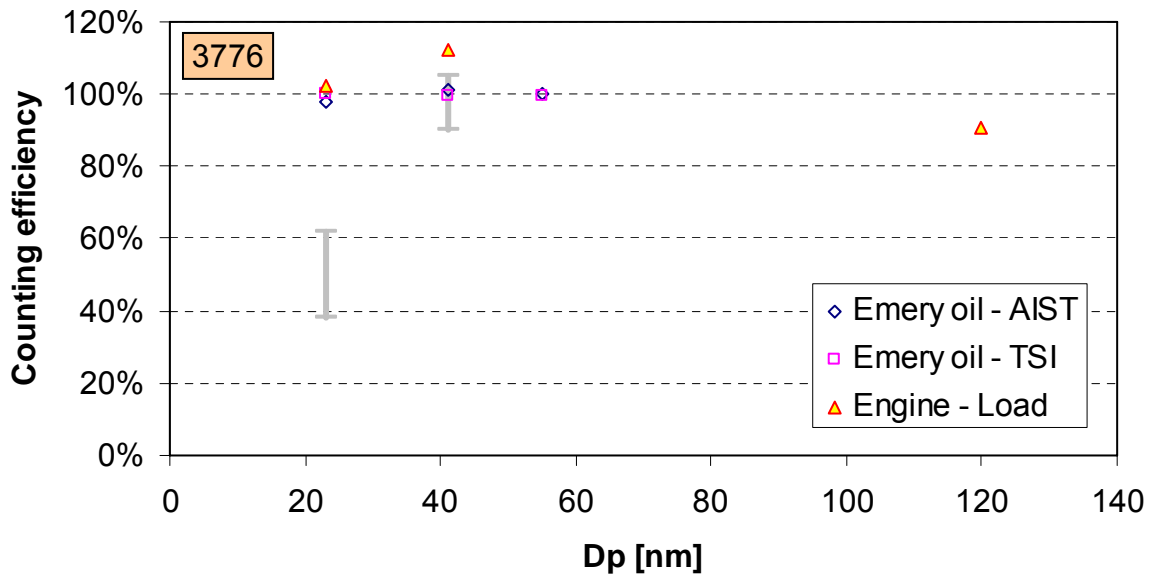


Figure 19: Counting efficiency of PNC 3776 (Reference).

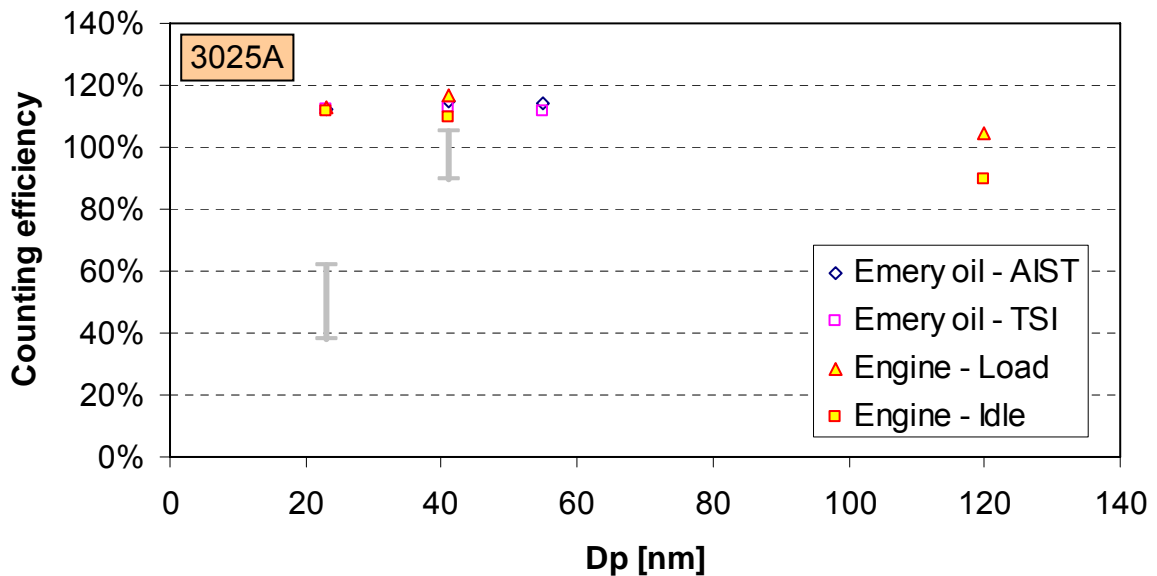


Figure 20: Counting efficiency of PNC 3025A.

4.2 Secondary method

According to the secondary method, the PNCs under evaluation are compared with a calibrated PNC. In the TSI case the reference PNC was PNC 3776 (with $d_{50} < 10$ nm). No correction was applied to the Reference PNC at the following results. This correction should be ~ 1 (see Table 21) depending on the material of the primary calibration of the specific PNC.

Linearity

Table 28: PNC JRC 3790

<i>Material</i>	<i>Slope</i>	<i>R2</i>	<i>1 – Difference</i>	<i>±CoV</i>
Emery oil - TSI	0.987	1.0000	0.988	0.3
Emery oil -AIST	0.959	0.9999	0.964	0.7
Engine load	0.989	0.9993	1.009	4.6

Counting Efficiency

The counting efficiency according to the secondary method is checked by comparing the concentrations of the PNC under calibration with the reference PNC (at various diameters). The counting efficiency of the reference PNC at the particular diameters must be taken into account. In the results presented below the counting efficiency of the Reference PNC 3776 was considered 1 at 23 and 41 nm. No correction was applied for the slope (a correction ~ 1 should be applied depending on the material).

Table 29: PNC JRC 3790

<i>Material</i>	<i>23 nm</i>	<i>CoV</i>	<i>41 nm</i>	<i>CoV</i>
Emery oil - TSI	0.730	1.2%	0.989	1.6%
Emery oil -AIST	0.561		0.926	
Engine load	0.581	1.9%	0.900	2.6%

PNC JRC 3790 had a slope ~ 0.98 and $R^2 > 0.999$ (0.97 required). The slope and the 1-Difference had similar values. The CoV of difference was $< 5\%$. In general, the results were similar with the primary method. The counting efficiencies as calculated with the primary and secondary method were also similar, confirming that the two methods give equivalent results.

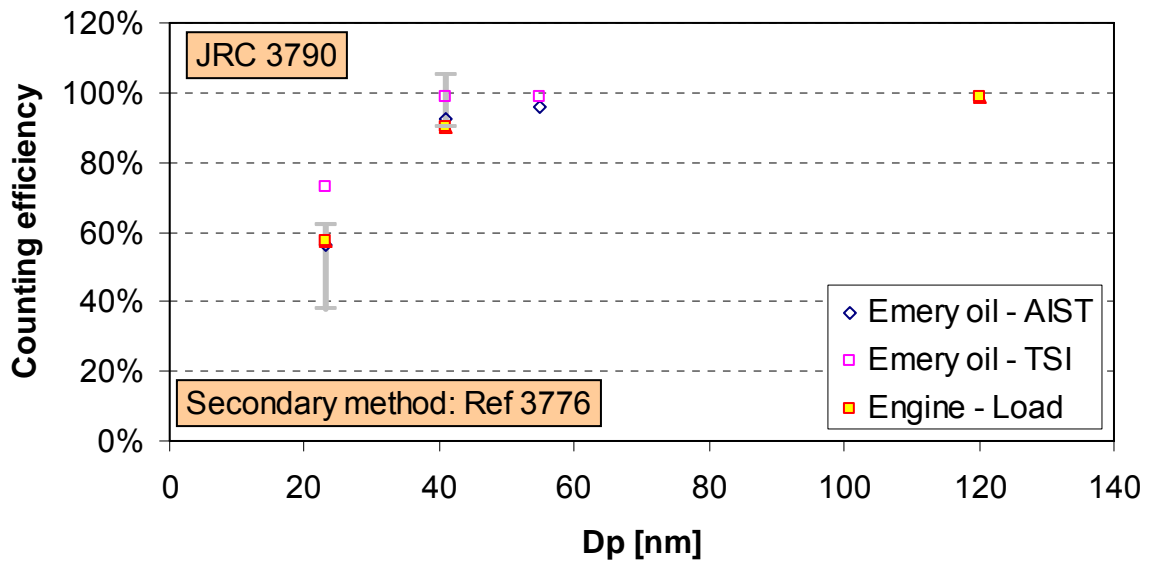


Figure 21: Counting efficiency of PNC JRC 3790 according to the secondary method.

5. DISCUSSION

So far the results for the specific PNCs were discussed. In the following sections more general issues will be discussed concerning the anticipated measurement uncertainties:

- Stability of the measurements during one day
- Repeatability of the measurements at the same lab during different days
- Reproducibility of the measurements at different labs with instruments of the same company
- Comparability of measurements with instruments of different companies

The above mentioned uncertainties will be discussed for the generators, the electrometers, the linearity and counting efficiency measurements. The results during this workshop will also be compared with other measurements at other labs.

5.1 Particle generators and material

One of the objectives of this workshop was to study the PNC efficiency and linearity dependence on aerosol materials. There are two aspects that need to be considered: the particle property and the generation method (Wang et al. 2007). The ideal material should have the following properties:

- Particle property
 - morphology (known preferred, e.g. spherical)
 - chemical composition (relevance to particles to be measured, no decomposition and evaporation)
 - low toxicity
 - monodispersity, few multiple-charged particles mixed
- Generation method
 - stable, compact, inexpensive generator
 - easy to operate
 - wide size and concentration range

Table 30 compares different materials used in this workshop concerning these aspects.

The engine exhaust particles were particles directly from engine and are most closely related to the real engine exhaust measurement. However, using these particles for PNC calibration causes several challenges: very limited size and concentration adjustability, large multiple charge fractions and aerosol property dependence on engine conditions, fuel,

lubricant etc. The engine exhaust data at idle mode during this workshop turned out to be an outlier.

The C40 and salt particles had limited size adjustment capabilities.

Electrospray generated emery oil particles had the advantage of being spherical, low multiple charge contamination (Table 6, Table 17), wide size and concentration range.

The CAST particles had small amount of doubly charged fractions and were easily generated with no additional requirements that have to be followed (e.g. radioactive source).

It is interesting to note the diesel particles had similar counting efficiencies with emery oil (oil) and CAST (aggregates). Thus, it can be assumed that the counting efficiencies of other diesel particles produced with other engines and/or fuels should be in the same range.

Table 30: Characteristics of particle generators.

<i>Material</i>	<i>Emery oil</i>	<i>C40</i>	<i>Diesel engine soot</i>	<i>NaCl</i>	<i>CAST Soot</i>
<i>Generator</i>					
Model	EAG	prototype	JRC engine	prototype	CAST
Concentration Stability	good	good	poor	good	good
Concentration Range	good	good	poor	good	good
Easy to operate	good	good	good	good	good
Cost	medium	low	very high	low	medium
<i>Generated Particles</i>					
Morphology	spherical	spherical	agglomerates	cubic/quasi-spherical	agglomerates
Relevance to	lube oil	lube oil	engine exhaust	atmospheric	combustion
Multiple charge ϵ	good	medium	poor	poor	medium
Toxicity	mild	mild	medium	low	medium
Size stability against evaporation and decomposition	semi-volatile	semi-volatile	medium	good	good
Size	> 4 nm	> 10 nm	> 10 nm	> 30 nm	> 10 nm

5.2 Multiple charge effect

The effect of the multiple charged particles was investigated with the term ε (ratio of doubly to singly charged particles, Eq. 1). Initially it was investigated what is the effect of the size distribution that enters the DMA on the term ε and then the effect of ε on the counting efficiencies.

5.2.1 Size distributions and ε

Figure 22 shows the multiple charge effect (ε) of various size distributions (the mean is given on the x axis and the σ on the chart) for measurement of 23, 41 and 70 nm monodisperse particles. It can be observed that the lower the mean diameter of the size distribution of the size distribution the lower the ε due to the lower fractions of doubly charged particles at smaller diameters. Also, the lower the σ , the lower the ε . In the same figure the experimentally defined ε (Table 17) is given for some tests, which confirm the trends.

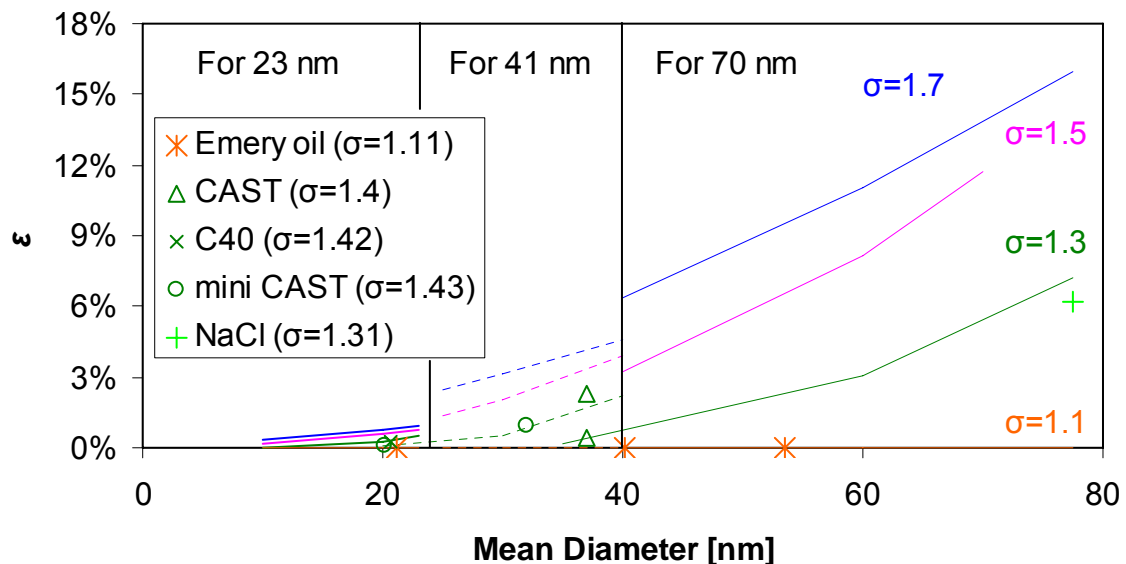


Figure 22: Effect of size distributions entering DMA on multiple charge effect on the monodisperse particles

5.2.2 Effect of ε on counting efficiencies

Table 31 summarises the effect of multiple charge (ε) on the measured counting efficiencies $c_{1,m}$ (without any multiply charged effect correction, e.g. Eq. 8). The multi-charge effect was identified according to the procedure described in section 2.4. As it can be seen, the higher the ε (higher contribution of multiple charged particles) the higher the effect on the counting efficiency c_1 . However, the effect depends also on the counting efficiency of the PNC under calibration (c_1). This can be easily understood, as the effect of ε on the PNC depends on the counting efficiency of the PNC (c_1) (Eq. 5), while the effect on the AE depends only on ε (Eq. 6). Figure 23 shows this relationship. In parallel, with the measured data from Table 31 the theoretical effect of four counting efficiencies are shown. For counting

efficiency of 0.5 the effect of ε on the counting efficiency is zero as the effects on the PNC and the AE cancel out. For higher counting efficiencies, the counting efficiency is underestimated without the multi-charge correction. For lower than 0.5 efficiencies, the counting efficiency is overestimated without the multi-charge correction. However, for all cases, the effect is negligible for $\varepsilon < 1\%$. This is even more clear in Figure 24 where it is shown that the higher the ε the higher the effect on the counting efficiency. For high counting efficiencies (e.g. during the linearity checks where the PNCs should have a value of 1) the counting efficiency error is close to 10% with ε of 10%.

Table 31: Summary of measured multiple charge effect on the electrometer AE, PNCs and counting efficiencies.

d_1 [nm]	Material	PNC	Conc. 2V n_2/n_1	ε (Eq. 1)	$c_{1,m}$ (Eq. 8)	$c_1/c_{1,m}$ (Eq. 4)
23	C40	TSI 3790	21%	0.24%	0.625	100.1%
23	C40	3010D	21%	0.24%	0.577	100.0%
23	C40	JRC 3790	21%	0.24%	0.862	100.2%
23	mini CAST	TSI 3790	141%	1.61%	0.159	92.3%
23	mini CAST	3010D	141%	1.61%	0.142	91.0%
23	mini CAST	JRC 3790	141%	1.61%	0.522	99.9%
23	CAST	TSI 3790	202%	2.32%	0.400	98.5%
23	CAST	3010D	202%	2.32%	0.026	52.8%
23	CAST	JRC 3790	202%	2.32%	0.544	100.0%
23	Engine idle	TSI 3790	978%	12.36%	0.873	109.4%
23	Engine idle	JRC 3790	978%	12.36%	1.116	112.8%
23	Engine idle	3025A	978%	12.36%	0.835	108.8%
23	Engine load	3776	251%	3.80%	0.988	103.5%
23	Engine load	3025A	251%	3.80%	1.129	104.0%
23	Engine load	JRC 3790	251%	3.80%	0.573	100.5%
23	Emery oil	3776	0.8%	0.01%	1.003	100.0%
23	Emery oil	JRC 3790	0.8%	0.01%	0.724	100.0%
23	Emery oil	3025A	0.8%	0.01%	1.121	100.0%

d_1 [nm]	Material	PNC	Conc. n_2/n_1	2V	ε (Eq. 1)	$c_{1,m}$ (Eq. 8)	$c_1/c_{1,m}$ (Eq. 4)
41	C40	TSI 3790	3%		0.14%	0.975	100.1%
41	C40	3010D	3%		0.14%	0.907	100.1%
41	C40	JRC 3790	3%		0.14%	1.020	100.1%
41	mini CAST	TSI 3790	2%		0.09%	0.734	100.0%
41	mini CAST	3010D	2%		0.09%	0.685	100.0%
41	mini CAST	JRC 3790	2%		0.09%	0.906	100.1%
41	CAST	TSI 3790	40%		2.35%	0.915	101.9%
41	CAST	3010D	40%		2.35%	0.640	100.7%
41	CAST	JRC 3790	40%		2.35%	0.950	102.0%
41	Engine idle	TSI 3790	80%		4.82%	0.918	104.0%
41	Engine idle	JRC 3790	80%		4.82%	1.095	104.9%
41	Engine idle	3025A	80%		4.82%	0.896	103.8%
41	Engine load	3776	134%		9.66%	1.021	109.1%
41	Engine load	3025A	134%		9.66%	1.168	110.4%
41	Engine load	JRC 3790	134%		9.66%	0.919	108.0%
41	Emery oil	3776	0.3%		0.02%	0.995	100.0%
41	Emery oil	JRC 3790	0.3%		0.02%	0.972	100.0%
41	Emery oil	3025A	0.3%		0.02%	1.128	100.0%

d_1 [nm]	Material	PNC	Conc. n_2/n_1	2V	ε (Eq. 1)	$c_{1,m}$ (Eq. 8)	$c_1/c_{1,m}$ (Eq. 4)
70	C40	TSI 3790	22%		3.58%	0.924	103.0%
70	C40	3010D	22%		3.58%	0.887	102.8%
70	C40	JRC 3790	22%		3.58%	0.950	103.1%
50	mini CAST	TSI 3790	12%		0.97%	0.845	100.7%
50	mini CAST	3010D	12%		0.97%	0.778	100.6%
50	mini CAST	JRC 3790	12%		0.97%	0.976	100.9%

80	NaCl	TSI 3790	32%	6.56%	0.833	113.5%
80	NaCl	3010D	32%	6.56%	0.788	113.1%
80	NaCl	JRC 3790	32%	6.56%	0.832	113.5%
60	CAST	TSI 3790	4%	0.44%	0.920	100.4%
60	CAST	3010D	4%	0.44%	0.786	100.3%
60	CAST	JRC 3790	4%	0.44%	0.925	100.4%
120	Engine idle	TSI 3790	10%	3.28%	0.829	102.3%
120	Engine idle	JRC 3790	10%	3.28%	0.953	102.8%
120	Engine idle	3025A	10%	3.28%	0.827	102.3%
120	Engine load	3776	28%	9.86%	0.946	108.5%
120	Engine load	3776	28%	9.86%	0.850	107.2%
120	Engine load	3025A	28%	9.86%	1.093	110.0%
120	Engine load	3025A	28%	9.86%	1.066	109.7%
120	Engine load	JRC 3790	28%	9.86%	0.926	108.2%
120	Engine load	JRC 3790	28%	9.86%	0.906	108.0%
55	Emery oil	3776	0.1%	0.01%	0.983	100.0%
55	Emery oil	JRC 3790	0.1%	0.01%	0.971	100.0%
55	Emery oil	3025A	0.1%	0.01%	1.109	100.0%

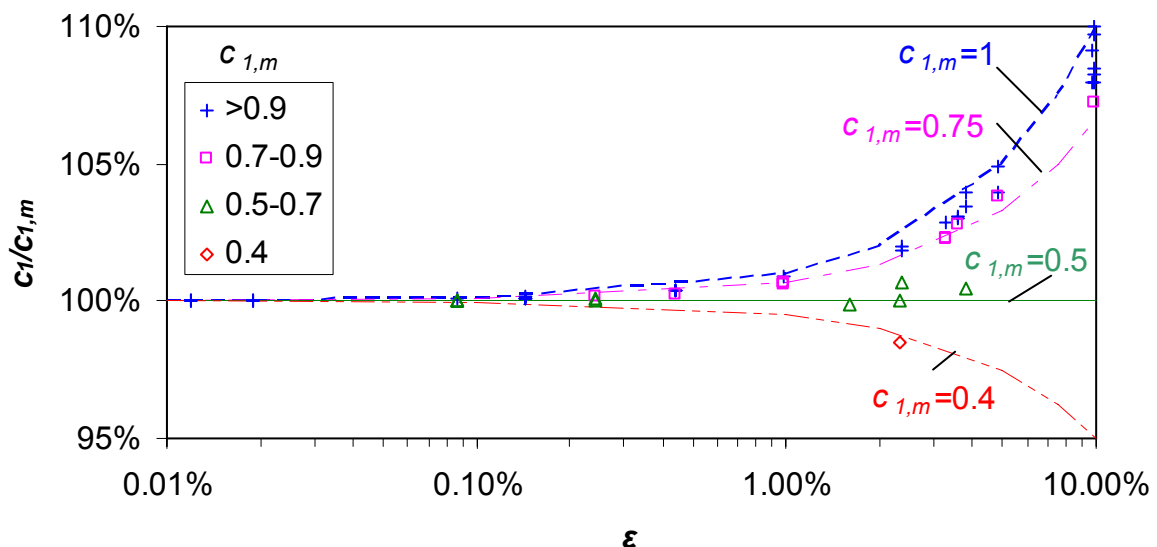


Figure 23: Effect of doubly charged particles on counting efficiency (primary method).

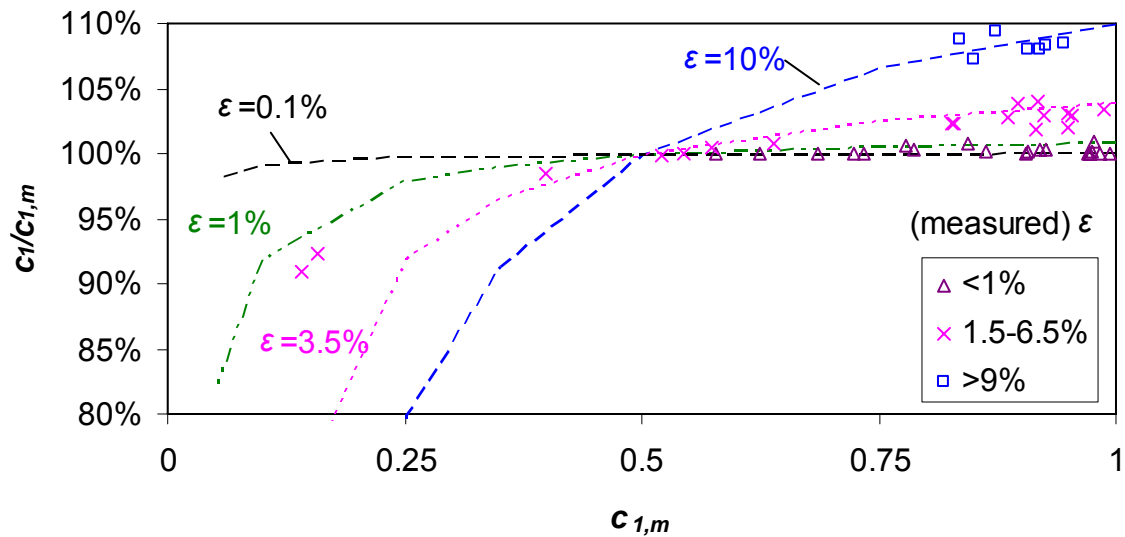


Figure 24: Effect on the measured PNC counting efficiency ($c_{1,m}$) of different multi-charge errors (ϵ).

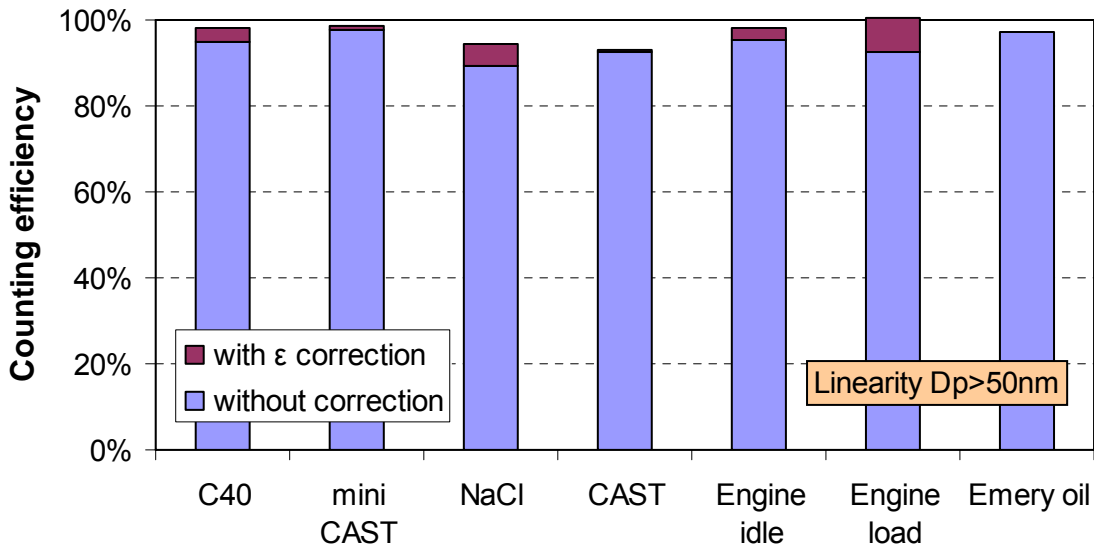


Figure 25: Effect of doubly charged particles on linearity tests of PNC JRC 3790.

Figure 25 shows the effect of the multiply charged particles on the linearity tests of the JRC 3790 counter as an example. With the correction the slopes come closer (from 0.89-0.98 to 0.93-1.00). It is therefore important to reduce the effects of multiply charged particles during PNC calibration. This can be achieved by choosing a generator that produces narrow distribution particles and selecting the calibration size from the right hand side of the particle size distribution. However if these are not possible, the multiple charge correction is necessary to be performed.

The effect of the ϵ on the counting efficiencies with the secondary method can be seen in Figure 26. In this case the reference PNC was considered that has counting efficiency 1. As it can be observed there is always an overestimation of the counting efficiency due to the doubly charged particles. The lower the counting efficiency of the test PNC, the higher the error. For a measured counting efficiency of 0.5 and ϵ 3% the “correct” counting efficiency is 5% lower. If the reference PNC has lower than one counting efficiency the effect of the multiply charged particles decreases as the errors cancel out.

It should be emphasized that at this study the concentration (during the linearity tests of the primary and secondary methods) was changed by changing the dilution. However, it is permitted to change the concentration downstream the DMA by changing the voltage (thus the diameter of the particles exiting the DMA as long as $d > 50$ nm). This effect was examined by considering a size distribution with mean around 45 nm and then estimating the ϵ for diameters 50-100 nm (Figure 27). The difference of ϵ between 50 and 100 nm is 2%. This means that when low concentration are measured (100 nm) the error of the measured counting efficiency will be 2% (for $c=1$, see Figure 23). For different size distributions the difference of ϵ between 50 and 100 nm will be different; usually less. However, this effect is the same for both CPCs, and if the test CPC has counting efficiency of 1, the errors cancel out (see Figure 26). So the two methods are equivalent.

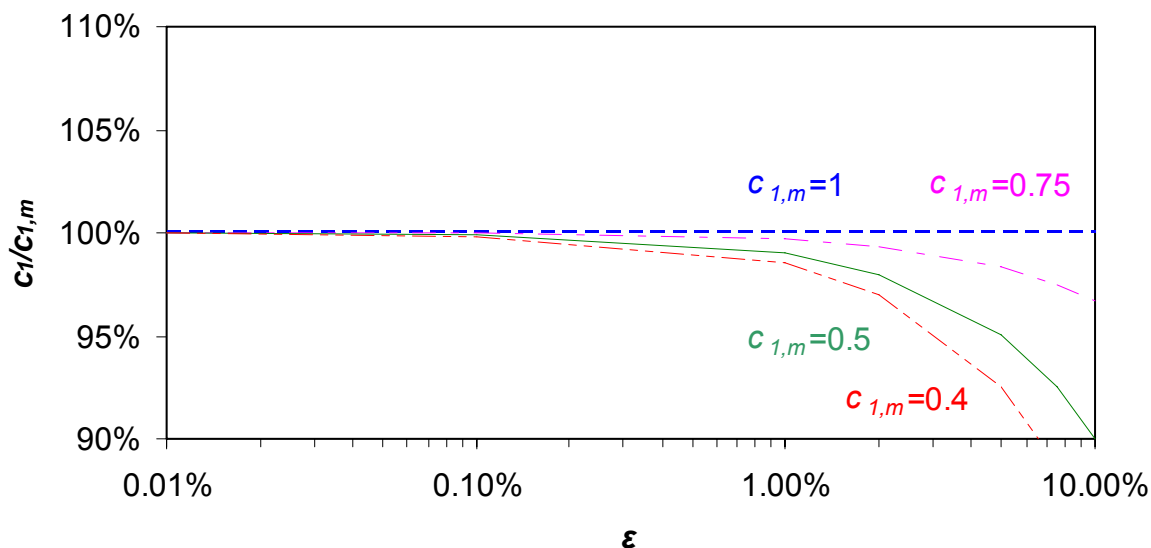


Figure 26: Effect of doubly charged particles on counting efficiency at the secondary method.

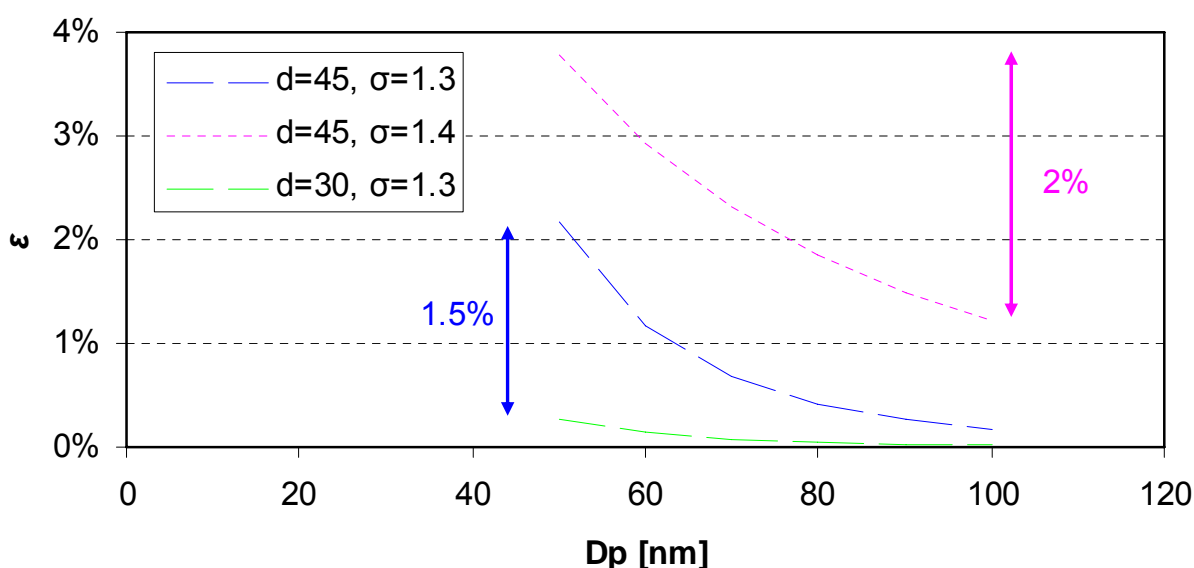


Figure 27: Effect of changing the concentration by changing the volate at DMA (thus the particle diameter).

5.3 Electrometers

5.3.1 Electrometers stability

One main source of data uncertainty is the aerosol electrometer: zero drift, flow accuracy and instrument status.

The flow rate was only measured once at the beginning of the workshop. The flow might have changed over the course of the workshop, which might have introduced some uncertainties.

Ideally, an aerosol electrometer needs to be turned on for a few days after shipping for the electronic circuit to stabilize. This was not possible during this workshop, and the TSI electrometer consistently read $\sim 7.3\%$ higher than the PNC 3776.

A well conditioned TSI 3068B AE has ± 1 fA RMS noise at 1 second averaging time (± 375 at the flow rate of 1 lpm used in the workshop). The AE used in the workshop seemed to satisfy this specification most of the time. An example of stable AE zero current with a HEPA filter at inlet is shown on the left side of Figure 28. However, it was noticed that when sampling engine exhaust, the AE drifted more than normal as depicted in the right side of Figure 28. This was probably due to the water and organic vapour in the engine exhaust which caused AE noise and current leakage. Even a ± 2 fA variation can introduce an uncertainty of ± 750 cm^{-3} which translates to an error of $\pm 20\%$ (as the measurements were conducted with particle concentrations ~ 4000 cm^{-3}). In the case of the engine idle case this error was 30% as the measured concentration was 2500 cm^{-3} . In case of drift, the AIST procedure will account for the AE drift more accurately, and will give more accurate results. Unfortunately, the AIST procedure was only followed once for emery oil measurement due to tight schedule. If longer experimental time was allowed, the AIST method would be preferred. The AIST procedure and TSI procedure would be equivalent if the aerosol electrometer had no zero drift.

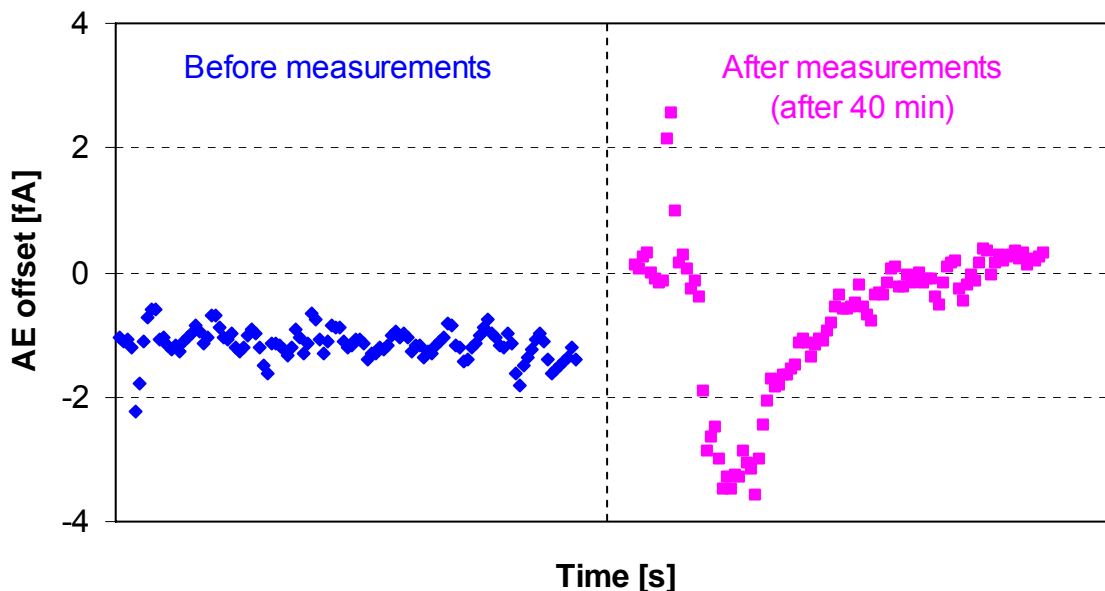


Figure 28: AE zero drift during the engine idle mode measurement. The time between these two measurements was ~ 40 minutes. Note that the AE was not very stable after the experiment and the mean value had drifted.

5.4 GRIMM-TSI comparability

The comparison of the GRIMM and TSI electrometers when measuring in parallel (see paragraph “GRIMM-TSI comparison” of the experimental set up) for 23 and 41 nm can be seen in Figure 29. The concentrations measured were very close (GRIMM measured 5% and 1% higher respectively). This means that the calibration constants of PNCs of the two companies have a <5% difference.

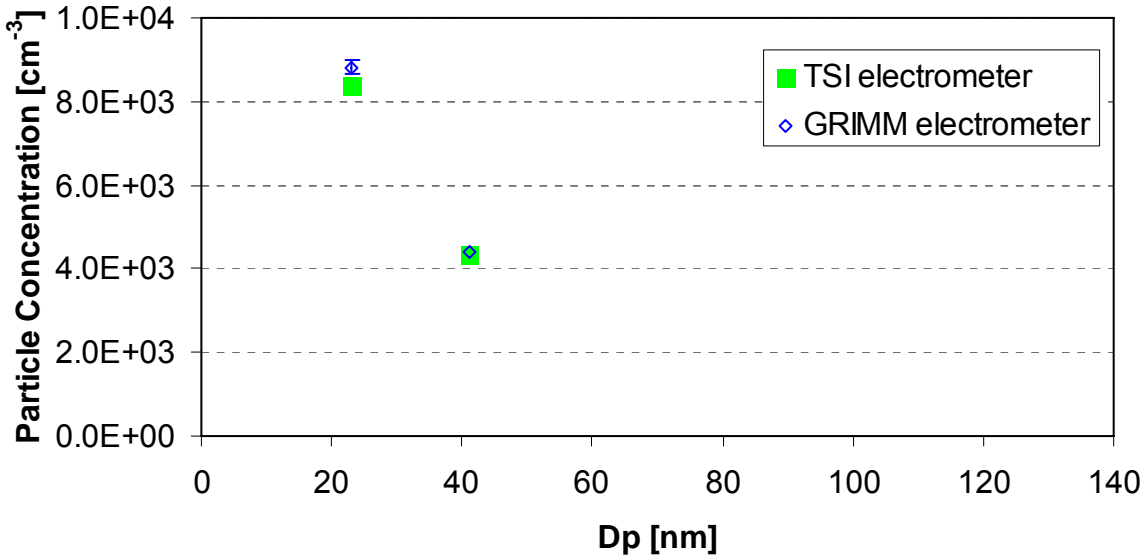


Figure 29: Comparison of TSI and GRIMM electrometers.

5.4.1 Size distributions

Direct comparison of the GRIMM and TSI size distributions was not possible as:

- The measurements were not always conducted simultaneously
- The sampling lines were of different lengths and diameters resulting in different losses and coagulation.
- The dilution used from each company was different.

Nevertheless the TSI size distributions showed modes at slightly higher peaks.

5.5 Linearity and counting efficiency uncertainties

5.5.1 Repeatability

During the GRIMM-TSI comparison tests the same instrumentation (JRC 3790, AE, GRIMM 608, FCE) was used as during the previous days. Thus, the results from the TSI-GRIMM comparison were also used to check the repeatability of the measurements.

For PNC JRC 3790 the results of the comparison and Table 23 should be similar as the same electrometer was used (but GRIMM's DMA). Figure 30 shows the results. For the 41 nm, the same efficiency was measured. For the 23 nm, there was a 0.04 difference. These results indicate that the GRIMM's DMA diameters should be similar with those of TSI's DMA as the result of TSI were repeatable.

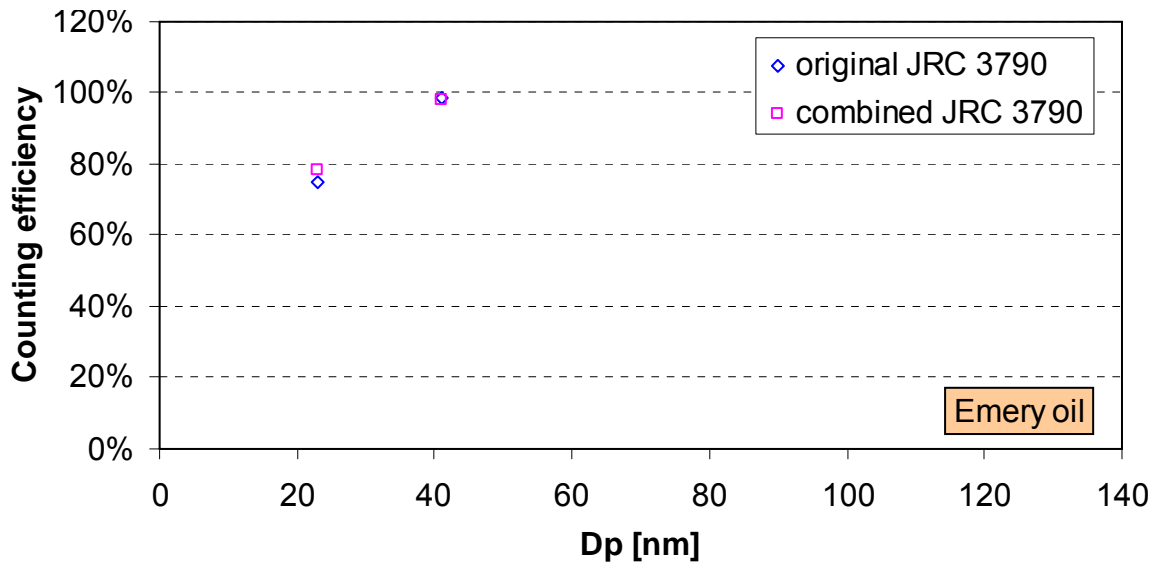


Figure 30: Repeatability of JRC 3790 counting efficiency measurements.

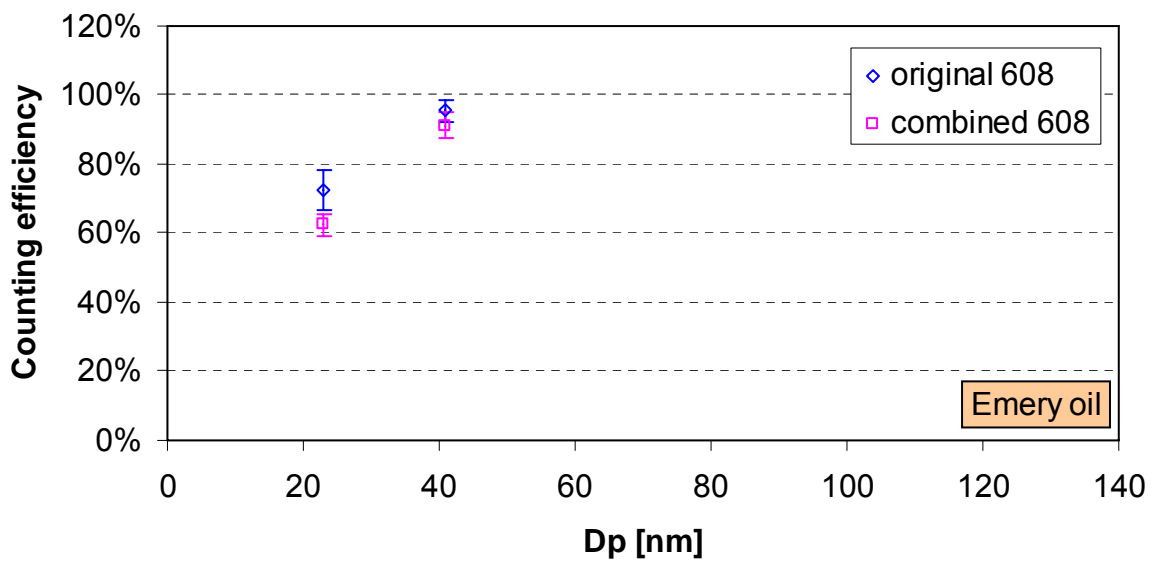


Figure 31: Repeatability of GRIMM 608 counting efficiency measurements.

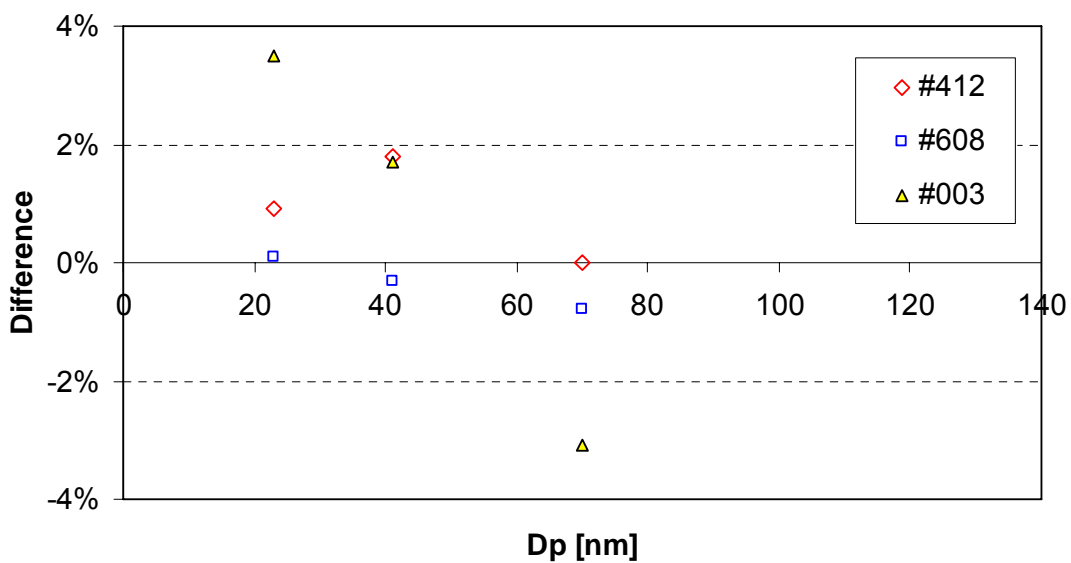


Figure 32: Repeatability of C40 particles with three GRIMM PNC counters (two days).

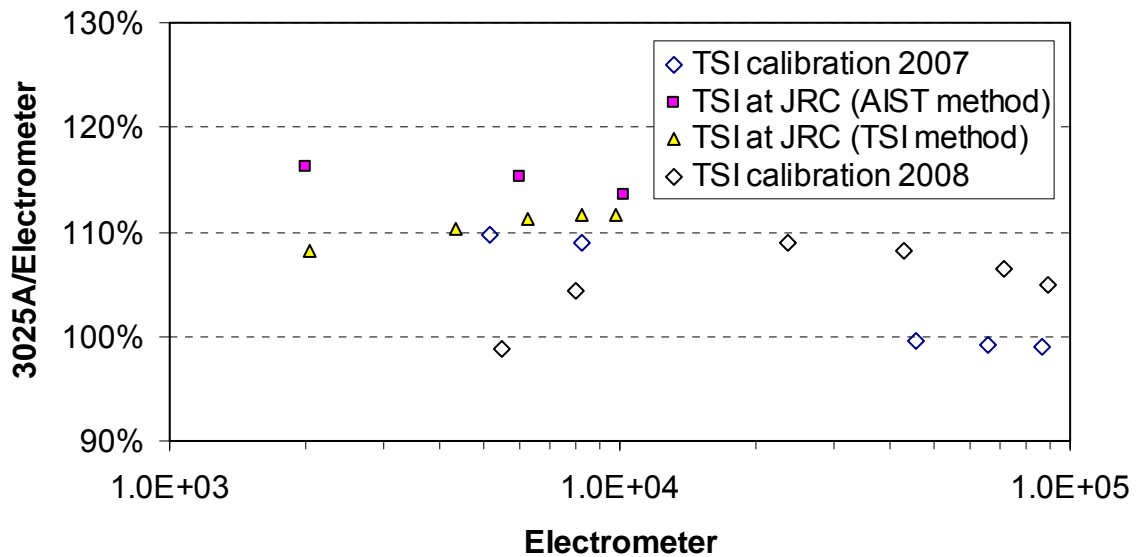


Figure 33: Reproducibility of linearity measurements (3025A).

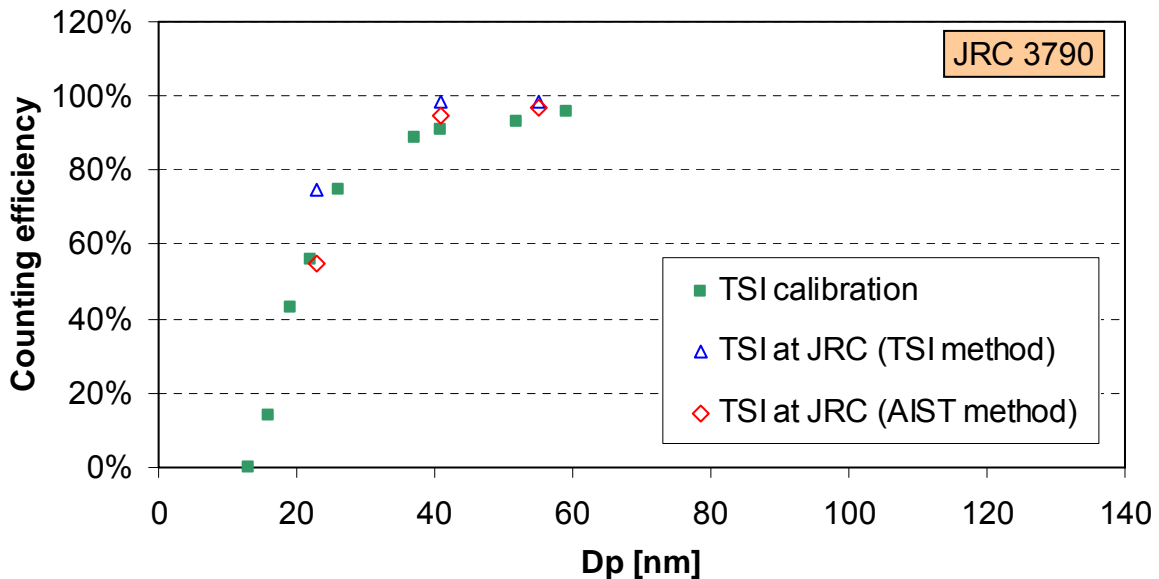


Figure 34: Reproducibility of counting efficiency measurements (JRC 3790).

For GRIMM PNC 608 the results of the comparison and Table 11 should be identical as the same DMA and the same electrometer were used. For the 41 nm, a 0.04 lower efficiency was measured. For 23 nm, 0.1 difference. These results also indicate that the cut-points determination repeatability is 0.05 (5%) for 41 nm and 0.1 (20%) for 23 nm.

The repeatability of the measurements was also checked by the GRIMM measurements with C40 particles at 2 different days. The results were given in Table 7-Table 12. Figure 32 shows the differences of the two days results. The differences at 70 nm particles correspond to the slope results. These results show that the expected uncertainty is within $\pm 4\%$.

5.5.2 Reproducibility

Non PMP PNC: The non-PMP PNCs are not calibrated for the counting efficiency, only for their linearity. The JRC 3025A (non-PMP) was calibrated from TSI before (1 Jun 07) and after the workshop (16 Sep 2008). The results can be seen in Figure 33 (TSI calibration). The

same PNC was also calibrated at the JRC workshop (5 Dec 07). The results of the two methods (TSI and AIST) are also given in the figure. These results show that the reproducibility uncertainty for the linearity constant should be within $\pm 5\%$.

PMP PNC: The slope for the JRC 3790 according to the original calibration was 0.932 (with emery oil). In this workshop it was found 0.95-0.97 (with emery oil). This $\sim 3\%$ difference indicates that a $<5\%$ reproducibility uncertainty should be expected. For the same PNC Figure 34 shows the original calibration (with emery oil) and the results of this workshop. The reproducibility uncertainty of the counting efficiencies is $<5\%$. However, at the slope higher uncertainty can be observed (up to 20%, i.e. 0.1 at the counting efficiency).

5.6 Comparison with JRC's measurements

Non-PMP PNC: The ratio of the 3025A to the GRIMM 003 was estimated from Table 9, Table 12, Table 22, Table 27 for emery oil (and taking into account the difference between the electrometers (1% at 23 nm, 5% at 41 nm and 5% at 55 nm)). These results were compared with a direct comparison of the two PNCs in JRC (9 Jul 07) with monodisperse NaCl particles. The results are in a very good agreement indicating that labs can safely use the secondary method for the check of their instrumentation.

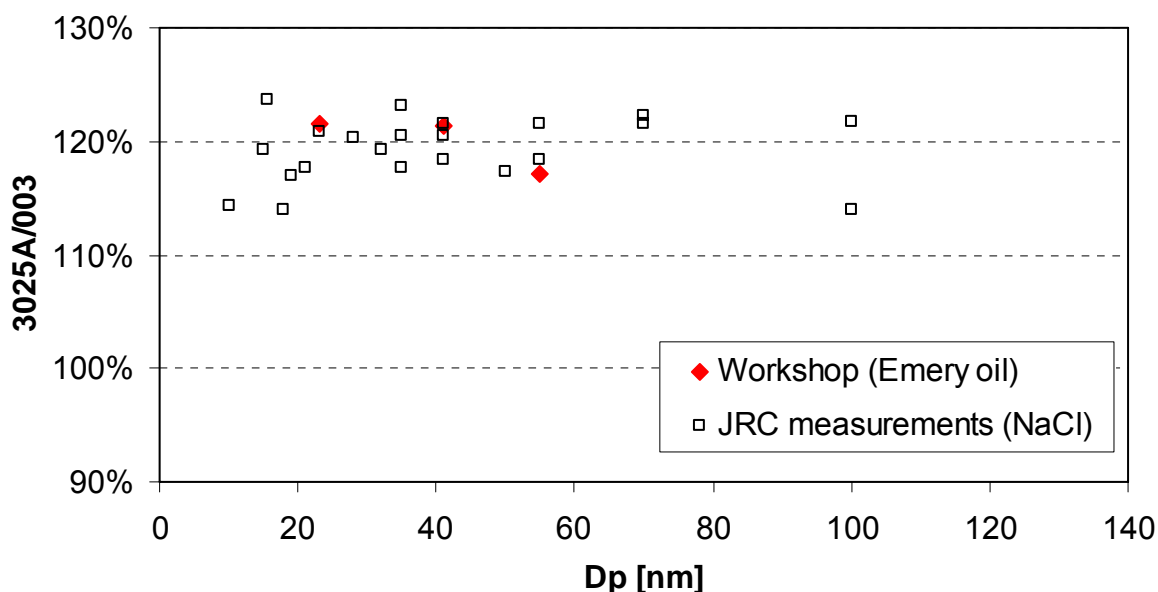


Figure 35: Comparison of 3025A and 003 during the workshop and previously in JRC.

PMP PNC: JRC two months before the calibration workshop conducted counting efficiency measurements, similar with those conducted in this workshop (02 Oct 07). In particular diesel particles were generated with the same engine at the same speed/torque conditions. Raw exhaust gas sampling was conducted with the same thermodenuder. The same electrostatic classifier was used but with the long column and not the nano column, which was used at the workshop.

The efficiency of the 3790 JRC PNC was checked with the secondary method (reference was the TSI 3025A PNC). It should be noted that the 13% difference between 3776 and

3025A was taken into account (see Table 21 and Table 22) (in the legend of the Figure 36 “3025A corr”). Figure 36 shows that the counting efficiencies measured by JRC and by TSI are in close agreement. These results show that the secondary method can be conducted by the labs without significant errors. However a 10% uncertainty should be expected from the labs at the determination of the cut-points (from the reported from the manufacturer value) even when using the same material.

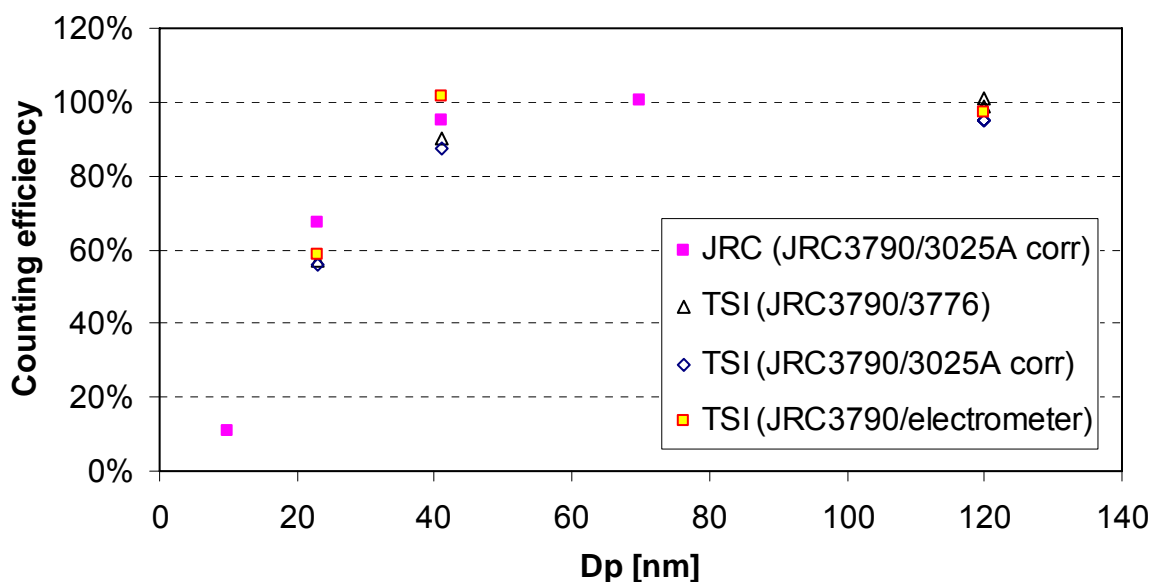


Figure 36: Counting efficiency measurements during the workshop and earlier at JRC for HD diesel particles.

5.7 Comparison with other studies

Figure 37 shows the counting efficiencies of a 3790 PNC for various materials. The data were taken during a TSI-AIST workshop in March, 2007 (Wang et al. 2007). NaCl was generated with a tube furnace, which gives a quite narrow distribution. The data were not correct for multiple charge effect as ϵ was only 1.17%.

Figure 38 shows the counting efficiency curve for the various materials from the two companies for two counters (TSI JRC 3790, GRIMM 608) which should have counting efficiency $50 \pm 12\%$ at 23 nm and $>90\%$ at 41 nm. Grey lines show the required from PMP counting efficiencies. The interaction between particles and the PNC working liquid is very important (e.g. C40 particles show high counting efficiency at 23 nm). CAST and emery oil particles give similar efficiencies, close to those measured with engine at medium load. The TSI-AIST workshop (Figure 37) showed that the PNC counting efficiencies are more highly dependent on the materials tested than at the JRC workshop. A complete picture of material dependence was out of this workshop’s scope.

Figure 39 compares the data from Figure 37 with the data from Figure 16 (or Figure 38) for two 3790 PNCs. For the two common aerosols (emery oil and NaCl), the findings of the two studies are consistent, although the 3790 PNCs used in the two studies were different.

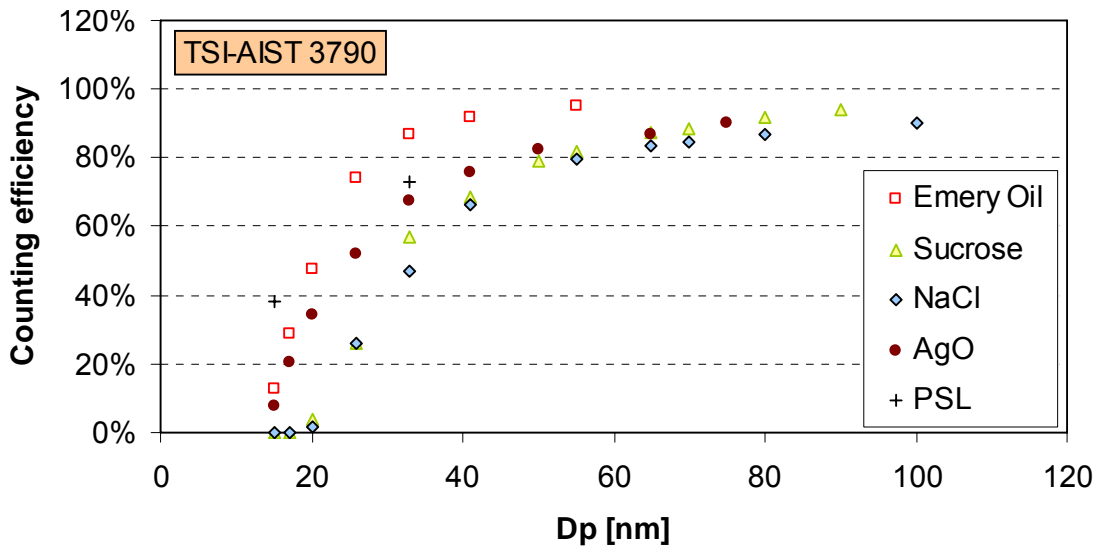


Figure 37: TSI-AIST workshop in March 2007 (Wang et al. 2007) for a PNC 3790.

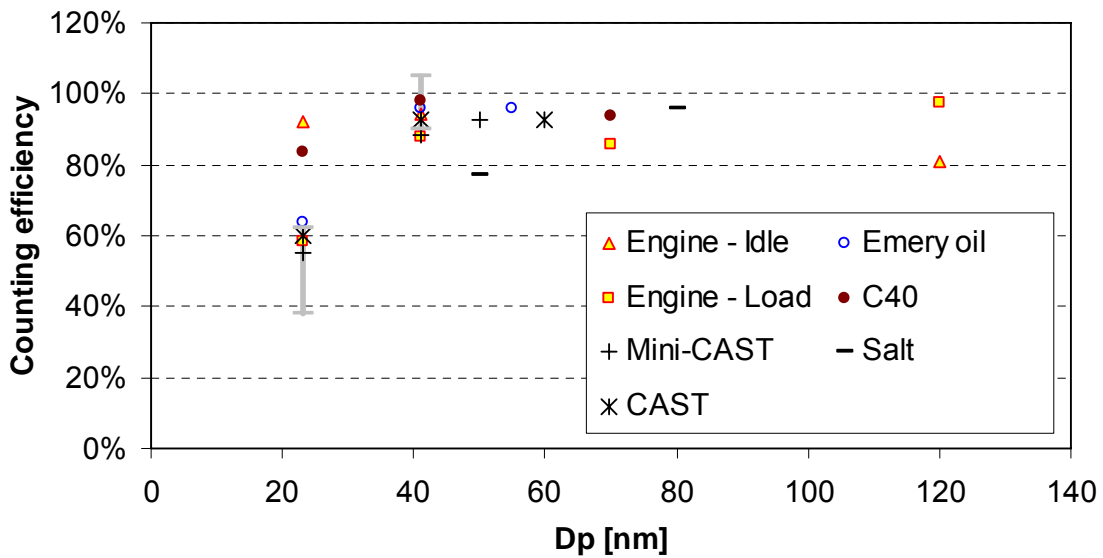


Figure 38: JRC workshop summary of material effect on two PMP PNCs.

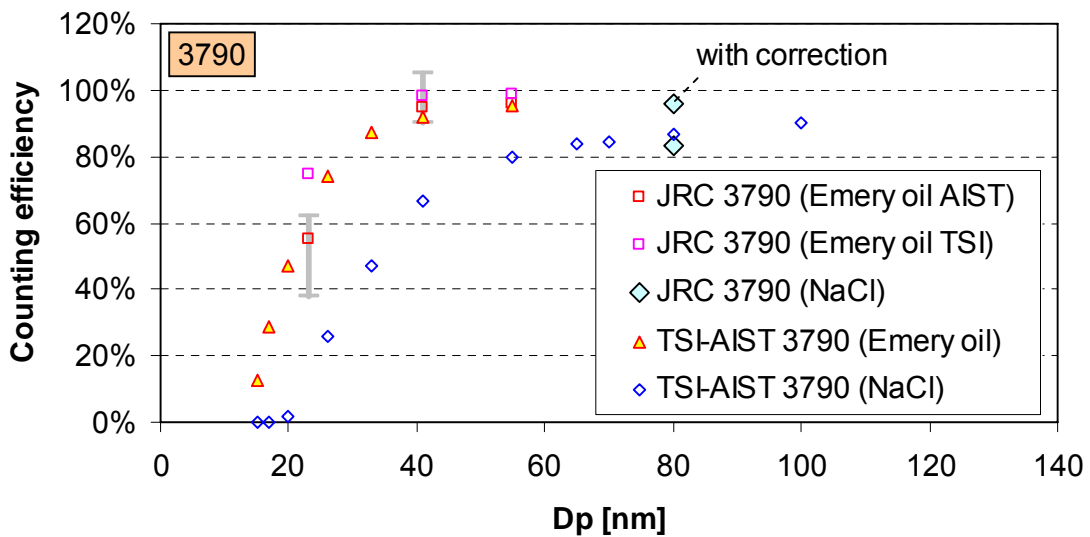


Figure 39: Comparison of TSI-AIST workshop results with JRC workshop results for two 3790 counters for emery oil and NaCl particles.

6. SUMMARY & CONCLUSIONS

Recently the particle number method was proposed to the light duty regulation, so the proper calibration of Particle Number Counters (PNCs) will be very important. Calibration includes the linearity measurement and the counting efficiency measurement. Labs will have to demonstrate compliance of their PNCs with a traceable standard within a 12 month period prior to the emissions test. Compliance can be demonstrated by:

- *Primary method:* By comparison of the response of the PNC under calibration with that of a calibrated aerosol electrometer when simultaneously sampling electrostatically classified calibration particles, or
- *Secondary method:* By comparison of the response of the PNC under calibration with that of a second PNC which has been directly calibrated by the above method.

Compliance testing includes linearity and detection efficiency with particles of 23 nm electrical mobility diameter. A check of the counting efficiency with 41 nm particles is not required.

A workshop was organised to investigate the effect of the material on the calibration procedures and the uncertainties of the suggested procedure. GRIMM and TSI provided PNCs (butanol based condensation particle counters) and AEA, MATTER, GRIMM, TSI provided five particle generators. The experiments were conducted in the European's Commissions laboratories (JRC). Heavy duty diesel engine (w/o after-treatment) particles were also produced (measurements downstream a thermodenuder) at idle and a medium load mode. The measured data were evaluated by JRC.

The main conclusions were:

Primary method:

Linearity

The material or size (when on the right hand side of the size distribution) dependence was small. However NaCl particles at 50 nm due to the low counting efficiency underestimated the slope. In addition, a high multi-charge effect of the NaCl distribution led to lower slope estimation.

The $R^2 > 0.997$ for all cases.

The differences between the electrometer and the PNCs under calibration at each concentration were usually lower than 10%. The 1-Difference was similar with the slope.

The CoVs of the differences were $< \pm 5\%$.

Counting efficiency

A material dependence on the counting efficiency was found. C40 particles showed higher efficiencies at 23 nm than the rest materials. CAST particles had similar efficiencies with diesel engine soot. Emery particles had also similar efficiencies or slightly higher.

The CoV of the measurements was generally <10% (mainly due to generators instability). With C-40 particles higher (due to generator instability).

Secondary method

Linearity

Slopes: The slopes were affected by the error of the slope of the Ref PNC. The effect of the multi-charged particles was much smaller than at the primary method. For a well calibrated PNC the differences with the primary method were less than 5%. If the slope of the reference PNC was taken into account, the primary and secondary methods were equivalent. The secondary method is highly recommended for labs that want to verify the proper operation of their PNCs.

The R2 values with the secondary method were >0.995.

The differences between the reference PNC and the PNCs under calibration at each concentration were usually lower than 10%. The 1-Difference was similar with the slope.

The CoVs of the differences were <5%.

It should be emphasised that at this study the concentration (during the linearity secondary method) was varied by changing the dilution. Theoretical calculations showed that the results should be similar with the method where the concentration varies by changing the voltage at the classifier (and consequently the diameter of the particles) for most cases (test CPC counting efficiency at these diameters 1).

Counting efficiency

Differences of up to 8% compared to the primary method were found. This error depended on the counting efficiency of the Reference PNC. If the counting efficiency of the reference PNC were taken into account, the primary and secondary methods were equivalent.

Uncertainties

Table 32 summarises the experimental uncertainties found during this workshop for the generation method, the electrometer and the linearity and counting efficiency methods. The stability of the measurements (mainly affected by the generator) is in the order of 10%. The repeatability of the measurements is in the order of 5%. The reproducibility of the measurements is in the order of 10%. However these percentages can be double at the measurements of 23 nm (the steep part of the counting efficiency curve).

Multiply charged particles effect

The multiply charged particles can increase the uncertainty of the measurement, and should be also considered. It was shown that the multi-charge effect should be taken into account when ϵ (ratio of doubly to singly charged particles) is >3%. This can result, for example, when a wide size distribution ($\sigma > 1.3$) is entering the DMA and big particles are measured (>40 nm).

Table 32: Uncertainties found during this workshop. Generator uncertainty is defined as the change of the peak concentration of the size distribution at the beginning and at the end of the tests (duration 20 min). The stability of the linearity and counting efficiency tests are calculated from the CoV of the ratio of the instruments.

	<i>Generator</i>	<i>Electrometer</i>	<i>Linearity</i>	<i>Counting Efficiency</i>
Stability	10% (Table 6)	<20%* (Figure 28)	±5% (Table 7-9, Table 18-22)	5-10% (Table 10-12, Table 23-26)
Repeatability	10% (Table 17)		±4% (Figure 32)	4% (Figure 30)
Reproducibility	-		±3% (5.4.2)	10% (5.4.2)
Comparability		±5% (Figure 29)		10%** (5.5)

* at extreme drift (e.g. with diesel engine particles)

** from secondary method (labs)

Key messages

Manufacturers (calibration)

The calibration should be conducted such as that the electrometer is corrected for all parameters (e.g. flow, zero, drift etc). The particle counter shouldn't be corrected for the flow as the slope (from the linearity check) will take this into account. The linearity and counting efficiency should be corrected for multiply charged effect (although it is desirable to use material with minimum effect).

Manufacturers should provide the following info for all PNCs:

Slope (0.9-1.1), R2 (>0.97), values of PNC and electrometer measured at each concentration tested and ratio of them (0.9-1.1).

Material used. In this workshop it was found that material like emery oil and CAST could easily be produced and used. In addition, they had similar counting efficiencies with the heavy-duty diesel particles at a medium load. For the rest materials more care should be taken.

Laboratories (validation)

Labs that check their PNCs should use the same material and the expected difference of the values reported by the manufacturer should be within 0.01 for the counting efficiency and 0.05 for the linearity checks. Multiply charged effect should be taken into account.

Primary and secondary methods were found equivalent. But the slope and the counting efficiencies of the Reference PNC should be taken into account.

7. REFERENCES

Amendments to UNECE Regulations, Regulation No. 83, Proposal for draft supplement 7 to the 05 series of amendments to Regulation No.83, ECE/TRANS/WP.29/GRPE/2007/8/Rev.1, <http://www.unece.org/trans/doc/2007/wp29grpe/ECE-TRANS-WP29-GRPE-2007-08r1e.pdf>.

Baron, P. and Willeke, K. (2005). *Aerosol Measurement: Principles, Techniques, and Applications*. Wiley-Interscience, John Wiley & Sons, 2nd edition

Hinds W. (1999). *Aerosol Technology: Properties, Behavior, and Measurement of Airborne Particles*. Wiley-Interscience, John Wiley & Sons, 2nd edition

Kulmala, M., Mordas G., Petaja T., Gronholm T., Aalto P. P., Vehkamäki H., Hienola A. I., Herrmann E., Sipila M., Riipinen I., Manninen H. E., Hameri K., Stratmann F., Bilde M., Winkler P. M., Birmili W. and Wagner P. E. (2007). The condensation particle counter battery (CPCB): A new tool to investigate the activation properties of nanoparticles. *J. Aerosol Sci.* 38, 289-304

Reischl, G. P., Mäkelä, J. M. & Nucid, J. (1997). Performance of a Vienna type differential mobility analyzer at 1.2-20 nanometer. *Aerosol Sci. Technology*, 27, 651-672

Wang, X., Sakurai, H., Hama, N., Caldow, R., Sem G.. (2007). Evaluation of TSI 3068B Aerosol Electrometer and 3790 Engine Exhaust CPC. Presented at 26th Annual Conference in Reno, NV, Sep. 24 - Sep. 28, 2007

Wiedersohler, A., H. J. Fissan (1988). Aerosol Charging in High Purity Gases. *J. Aerosol Sci.* 19: 867-870

Appendix: Specifications of emery oil

For more information and technical assistance contact:

Chevron Phillips Chemical Company LP
P.O. Box 4910
The Woodlands, TX 77387-4910
800.852.5531



Synfluid[®] PAO 4 cSt Highly Branched Isoparaffinic Polyalphaolefin

Application Synfluid[®] 4 cSt PAO can be used in many industrial and automotive lubricant applications. These include gear oils, compressor oils, engine oils, hydraulic fluids, greases, and other functional fluids.

Handling Maximum temperatures of 65 °C (149 °F) for handling and ambient for long-term storage are recommended. For specific instructions on handling, see MSDS.

Typical Properties

Property	Typical Value
Kinematic Viscosity, cSt @ 212°F, 100°C	3.9
Kinematic Viscosity, cSt @ 104°F, 40°C	16.8
Kinematic Viscosity, cSt @ -40°F, -40°C	2,420
Viscosity Index	124
Pour Point, °F, °C	-100 (-73)
Flash Point (COC), °F, °C	425 (219)
Fire Point (COC), °F, °C	480 (249)
Volatility, Noack, wt%	13.0
Specific Gravity, 60°/60°F, 15.6°/15.6°C	0.8190
Density, lb/gal	6.820
Total Acid Number	---
Bromine Index	<200
Appearance	Clear and Bright
Odor	No Foreign Odor
Color, Pt-Co	<1
Color, Saybolt	+30

MSDS #3332

Revision Date March, 2004

Another quality product from



Before using this product, the user is advised and cautioned to make its own determination and assessment of the safety and suitability of the product for the specific use in question and is further advised against relying on the information contained herein as it may relate to any specific use or application. It is the ultimate responsibility of the user to ensure that the product is suited and the information is applicable to the user's specific application. Chevron Phillips Chemical Company LP does not make, and expressly disclaims, all warranties, including warranties of merchantability or fitness for a particular purpose, regardless of whether oral or written, express or implied, or allegedly arising from any usage of any trade or from any course of dealing in connection with the use of the information contained herein or the product itself. The user expressly assumes all risk and liability, whether based in contract, tort or otherwise, in connection with the use of the information contained herein or the product itself. Further, information contained herein is given without reference to any intellectual property issues, as well as federal, state or local laws which may be encountered in the use thereof. Such questions should be investigated by the user.

European Commission

EUR 23495 EN– Joint Research Centre – Institute for Environment and Sustainability

Title: Calibration of PMP Condensation Particle Number Counters: Effect of material on linearity and counting efficiency.

Author(s): Giechaskiel B., Alessandrini S., Forni F., Carriero M., Krasenbrink A., Spielvogel J., Gerhart C., Wang X., Horn H., Southgate J., H. Jörgl, G. Winkler, L. Jing, M. Kasper

Luxembourg: Office for Official Publications of the European Communities

2008 – 62 pp. – 21 x 29.9 cm

EUR – Scientific and Technical Research series – ISSN 1018-5593

ISBN 978-92-79-09766-9

DOI 10.2788/95549

Abstract

Recently the particle number method was proposed to the light duty regulation, so the proper calibration of Particle Number Counters (PNCs) will be very important. Calibration includes the linearity measurement and the counting efficiency measurement. Labs will have to demonstrate compliance of their PNCs with a traceable standard within a 12 month period prior to the emissions test. Compliance can be demonstrated by:

-Primary method: By comparison of the response of the PNC under calibration with that of a calibrated aerosol electrometer when simultaneously sampling electrostatically classified calibration particles, or

-Secondary method: By comparison of the response of the PNC under calibration with that of a second PNC which has been directly calibrated by the above method.

Compliance testing includes linearity and detection efficiency with particles of 23 nm electrical mobility diameter. A check of the counting efficiency with 41 nm particles is not required.

A workshop was organised to investigate the effect of the material on the calibration procedures and the uncertainties of the suggested procedure. GRIMM and TSI provided PNCs and AEA, MATTER, GRIMM, TSI provided five particle generators. The experiments were conducted in the European's Commissions laboratories (JRC). Heavy duty diesel engine (w/o aftertreatment) particles were also produced (measurements downstream a thermodenuder) at idle and a medium load mode. The measured data were evaluated by JRC.

The results showed that there was an effect of the material used and suggestions were given. In addition the uncertainties of the procedure were quantified. Theoretical calculations showed the corrections that should be applied.

How to obtain EU publications

Our priced publications are available from EU Bookshop (<http://bookshop.europa.eu>), where you can place an order with the sales agent of your choice.

The Publications Office has a worldwide network of sales agents. You can obtain their contact details by sending a fax to (352) 29 29-42758.

The mission of the JRC is to provide customer-driven scientific and technical support for the conception, development, implementation and monitoring of EU policies. As a service of the European Commission, the JRC functions as a reference centre of science and technology for the Union. Close to the policy-making process, it serves the common interest of the Member States, while being independent of special interests, whether private or national.

